

Shell sclerochronology and stable isotopes of the bivalve *Anomalocardia flexuosa* (Linnaeus, 1767) from southern Brazil: Implications for environmental and archaeological studies



André Carlo Colonese^{a,*}, Sérgio Antônio Netto^b, André Silva Francisco^b, Paulo DeBlasis^c, Ximena S. Villagran^c, Raquel de Almeida Rocha Ponzoni^d, Y. Hancock^{d,e}, Niklas Hausmann^{a,f}, Deisi Sunderlick Eloy de Farias^g, Amy Prendergast^h, Bernd R. Schöne^h, Francisco William da Cruzⁱ, Paulo César Fonseca Gianniniⁱ

^a BioArCh, Department of Archaeology, University of York, Environment Building, Wentworth Way, York, YO10 5DD, UK.

^b Marine Science Laboratory, Universidade do Sul de Santa Catarina (UNISUL), Av J. Acácio Moreira, 787, Dehon, Tubarão 88704-900, Brazil.

^c Museu de Arqueologia e Etnologia, Universidade de São Paulo (USP), Av. Prof. Almeida Prado, 1466, Butantã, São Paulo 05508-070, Brazil.

^d Department of Physics, University of York, Heslington, York YO10 5DD, UK.

^e York Centre for Complex Systems Analysis, University of York, York YO10 5GE, UK.

^f Institute of Electronic Structure and Laser, Foundation for Research and Technology - Hellas, P.O. Box 1527, GR-711 10 Heraklion, Greece.

^g Grupep, Universidade do Sul de Santa Catarina (UNISUL), Av J. Acácio Moreira, 787, Dehon, Tubarão 88704-900, Brazil.

^h Institute of Geosciences, University of Mainz, J.-J.-Becher-Weg 21, 55128 Mainz, Germany.

ⁱ Instituto de Geociências, Universidade de São Paulo (USP), R. do Lago, 562, Cidade Universitária, São Paulo 05508-080, Brazil.

ARTICLE INFO

Article history:

Received 3 August 2016

Received in revised form 5 December 2016

Accepted 4 January 2017

Available online 6 January 2017

Keywords:

Eastern South America

Coastal lagoon

Anomalocardia flexuosa shells

Sclerochronology

Light stable isotopes

ABSTRACT

This study presents the first stable isotopic and sclerochronological calibration of the bivalve *Anomalocardia flexuosa* (Linnaeus, 1767) in relation to environmental variables in a subtropical coastal area of southern Brazil. We investigate incremental shell growth patterns and $\delta^{18}\text{O}$ and $\delta^{13}\text{C}$ values of modern specimens collected alive from the Laguna Lagoonal System (LLS). Shells of *Anomalocardia flexuosa* are also one of the main biological components of pre-Columbian archaeological shell mounds and middens distributed along the Brazilian coastline. We therefore selected archaeological specimens from a local late Holocene shell mound (Cabeçuda) to compare their stable carbon and oxygen isotope values with those of modern specimens. Shell growth increments, $\delta^{18}\text{O}$ and $\delta^{13}\text{C}$ values respond to a complex of environmental conditions, involving, for example, the effects of temperature and salinity. The isotopic information extracted from archaeological specimens from Cabeçuda shell midden in the LLS indirectly indicates that environmental conditions during the late Holocene were different from present day. In particular, intra-shell $\delta^{18}\text{O}$ and $\delta^{13}\text{C}$ values of archaeological shells reveal a stronger marine influence at 3 ka cal BP, which is in contrast to the seasonal freshwater/seawater balance that currently prevails at the LLS.

© 2017 Elsevier B.V. All rights reserved.

1. Introduction

Highly-resolved palaeoenvironmental information for tropical and subtropical coastal areas of South America predominantly come from pollen records, calcareous nanofossil assemblages and geomorphological evidence (e.g. Baker and Fritz, 2015; França et al., 2013; Gyllencreutz et al., 2010). Whereas these records provide robust palaeoclimate and palaeoenvironmental information spanning decadal to millennial timescales, there is still a need for archives resolving sub-annual environmental conditions (e.g. Carré et al., 2005; Yan et al., 2012). For example, data on intra-annual sea surface temperature and

biological productivity are crucial for assessing the impact of extreme ocean-atmosphere phenomena, such as the El Niño/Southern Oscillation, on local/regional hydrological and biological processes at seasonal time-scales (Aravena et al., 2014; Garcia et al., 2003; Stenseth et al., 2002). Furthermore, several lines of evidence point to considerable reorganisations of coastal ecosystems from the middle Holocene to present-day in response to relative sea-level changes in eastern South America (Angulo et al., 2006). In some tropical and subtropical areas geomorphological and palynological records reveal a marked retraction or disappearance of rich aquatic ecotones, such as estuaries and coastal lagoons, during this period (Carvalho do Amaral et al., 2012; Carvalho et al., 2004; Fornari et al., 2012; França et al., 2013). Although it is well known that present day human populations inhabiting these areas are extremely vulnerable to increasing climate and environmental

* Corresponding author.

E-mail address: andre.colonese@york.ac.uk (A.C. Colonese).

variability (Defeo et al., 2013; Magrin et al., 2007), the impact of these changes on human societies in the past remains largely unknown.

Aquatic mollusc shells are excellent archives for high resolution palaeoclimate reconstructions. During carbonate precipitation, mollusc shells register endogenous and environmental information in the form of geochemical signatures and structural characteristics spanning daily to annual time intervals (e.g. Goodwin et al., 2003; Schöne, 2008; Schöne and Surge, 2012). Mollusc shells can provide information on water temperature, hydrologic balance, productivity and ocean circulation (Dettman et al., 2004; García-March et al., 2011; Mannino et al., 2008; Milano et al., 2017; Prendergast et al., 2013; Schöne and Gillikin, 2013; Surge et al., 2003; Wanamaker et al., 2008). Moreover, many intertidal and subtidal species have been widely exploited by human populations in the past and thus their shells are often preserved in archaeological sites (Colonese et al., 2011; Erlandson, 2001; Gaspar et al., 2008), offering the opportunity to investigate past climate and environmental conditions in relation to human societies. Finally, many species exploited in the past are still economically relevant to present-day human societies (Bardach, 1997), as such an increasing knowledge of their physiology and ecology is vital for implementing appropriate management and assessment strategies.

In the present study we conduct the first stable isotopic and sclerochronological calibration of the bivalve *Anomalocardia flexuosa* (Linnaeus, 1767) in relation to environmental variables. We investigate incremental shell growth patterns and stable carbon and oxygen isotope composition of modern specimens collected alive from the Laguna Lagoonal System, in southern Brazil. *A. flexuosa* has considerable economic importance for present-day coastal communities along the subtropical and tropical Atlantic coasts of South America (Boehs et al., 2008; Gaspar et al., 2011; Silva-Cavalcanti and Costa, 2011). Its shells are also very abundant in pre-Columbian shell mounds locally known as *sambaquis* found in these regions (Gaspar et al., 2008). Thus, we also selected archaeological specimens from a local shell mound to compare their oxygen and carbon isotopic profiles with modern counterparts. Our main aim is to establish a new environmental proxy for subtropical coastal lagoon and estuaries in eastern South America, with a secondary aim of exploring seasonal environmental conditions in pre-Columbian times, during the expansion of sambaqui cultures.

1.1. Environmental and archaeological setting

1.1.1. Laguna Lagoonal System

The Laguna Lagoonal System (LLS) is located in the State of Santa Catarina, in the southern coast of Brazil (S 28°12' E 48°38'; Fig. 1). The study area has a temperate climate (Peel et al., 2007) with mean air temperatures around 13 °C in the winter (July) and 22 °C in the summer (January), and mean annual rainfall between 1250 mm, in the north, and 1400 mm, in the south (Orselli, 1986). The LLS is a choked lagoon complex (Kjerfve, 1994) composed of three lagoons covering an area of 184 km²: Mirim, in the north; Imaruí, the largest lagoon in the middle of the system; and Santo Antônio, in the south (Fig. 1). The LLS is connected with the adjacent ocean by a narrow inlet in the south eastern sector of the system (Entrada da Barra), at Santo Antônio Lagoon. Freshwater inputs derive from three main rivers (Tubarão, Duna and Aratingaúba), however the largest contribution is provided by Tubarão River with a drainage area of 4.728 km² and an average annual discharge of 50 m³/s (Fonseca and Netto, 2006), forming a lagoonal delta into Santo Antônio Lagoon (Giannini et al., 2010; Fornari et al., 2012). The Tubarão lagoonal delta has gradually silted the lagoon complex to the south of Santo Antônio Lagoon since the mid Holocene (Giannini et al., 2007, 2010; Fornari et al., 2012). A sand barrier delimits the LLS to the east, whereas the western side is bordered by the pre-Cenozoic crystalline rock basement, a geomorphological unit known as the Serra do Tabuleiro (Hesp et al., 2009). The mean depth of the lagoon is around 2 m, and circulation is driven by a complex interaction of wind, tide and freshwater discharge (Fonseca and Netto, 2006).

1.1.2. Early fisheries of Atlantic South America: the sambaquis

The coastal areas of eastern South America have supported human occupation at least since the middle Holocene (Lima et al., 2002) and from ca. 6 to 1.5 ka cal BP pre-ceramic coastal populations occupied the surrounding areas of the LLS. These groups were highly adapted to interact with a variety of coastal environments and left behind some of the world's largest shell mounds, or sambaquis (DeBlasis et al., 2007; Gaspar et al., 2008; Giannini et al., 2010). These sites are frequently stratified and predominantly composed of shells, notably of *A. flexuosa*, and fish bones (Villagran, 2014). Recent studies have attested

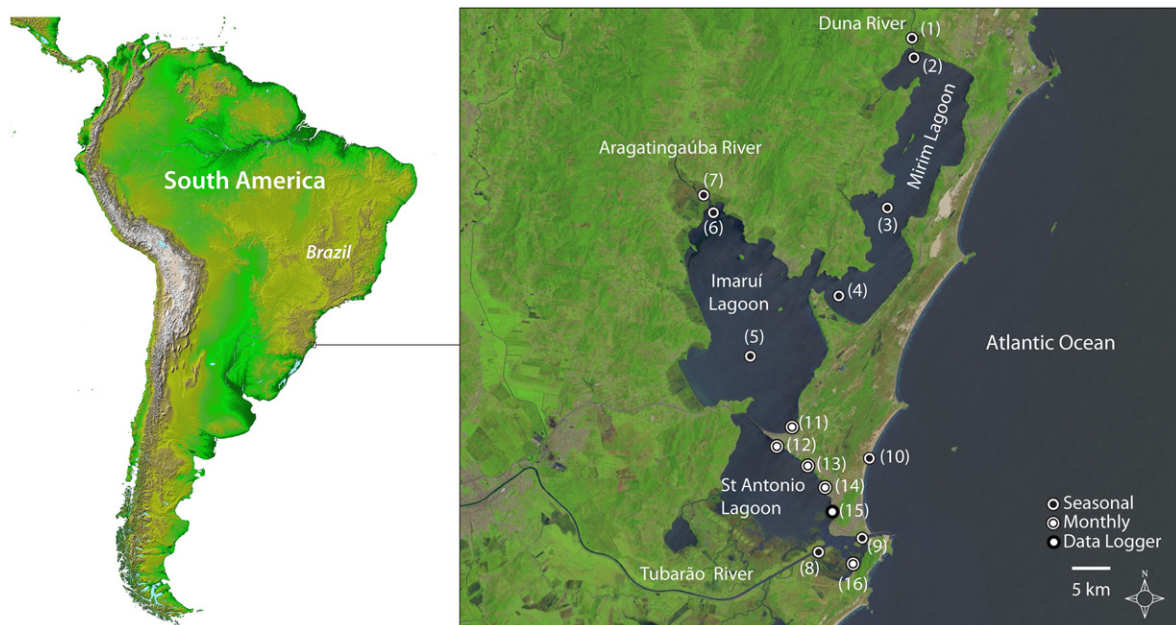


Fig. 1. Laguna Lagoonal System (LLS) in southern Brazil and the sample localities of instrumentally recorded salinity and temperature data, and $\delta^{18}\text{O}_\text{w}$ values. Living specimens were collected at localities 12, 13, 14 and 15. Archaeological specimens from Cabeçuda shell mound refers to locality 12. Surface salinity, temperature and $\delta^{18}\text{O}_\text{w}$ values were sampled to record the environmental gradient from freshwater to seawater endmembers. Satellite imagery from USGS (Earth Explorer) and NASA (Shuttle Radar Topography Mission).

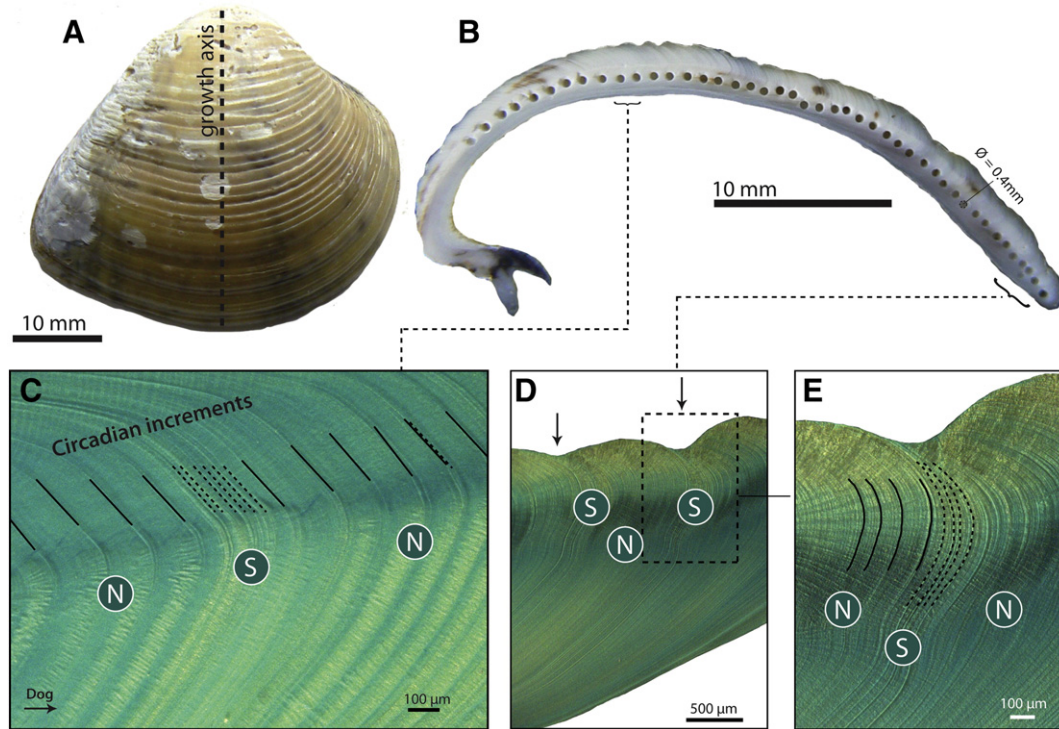


Fig. 2. A) Specimen AF-13-1 from locality 13; the dotted line represents the axis of maximum growth. B) Polished cross-section with manually sampled carbonates from the outer layer for stable isotope analyses. The pigmented areas are carotenoids. C–E) Details of polished cross-section immersed in Mutvei's solution showing distinct periodic microgrowth increments with variable width during neap (N, continuous line) and spring (S, dotted line) tides. The growth rate decreases with ontogenetic age, from the umbo toward the ventral margin. Dog: direction of growth.

that some sites were occupied for hundreds of years (Gaspar et al., 2008), with shells intentionally used as raw material for mound construction, which in some cases reached > 30 m high and several hundred meters in diameter (DeBlasis et al., 1998, 2007). The sambaquis had distinct functions, from burial sites (with hundreds of human burials) to dwelling structures (Villagran, 2014), and indirectly testify to a large-scale, long-term exploitation of coastal resources. Multidisciplinary studies confirm that the builders of the sambaquis were involved in fishing, especially in bays and coastal lagoons (Figuti, 1993; Villagran et al., 2011; Colonese et al., 2014; Bastos et al., 2015), and complemented their diet with plants and terrestrial mammal resources (Scheel-Ybert, 2001). Other elements of the material culture similarly invoke the reliance on marine resources, such as tools made of sea mammal and fish bones, as well as sophisticated zoomorphic sculptures representing aquatic animals (Gaspar et al., 2008). The emergence and maintenance of this long-term cultural practice required a deep understanding of coastal environmental conditions and their changes through time.

1.1.3. *Anomalocardia flexuosa*, Mollusca, Bivalvia, Veneridae

The bivalve *A. flexuosa* (Linnaeus, 1767), formerly known as *A. brasiliensis* (Gmelin, 1791), inhabits shallow subtidal and intertidal areas of transitional environments (e.g. estuaries, coastal lagoons) from the Caribbean to subtropical South America (e.g. Monti et al., 1991; Rios, 1994; Rodrigues et al., 2013; Silva-Cavalcanti and Costa, 2011). It occurs predominantly in fine sand or in a mixture of sand and mud substrates, and in the study area the species was observed only in the sandy sediments of the eastern portion of the Santo Antônio Lagoon. The species typically tolerates large variations in salinity (Leonel et al., 1983; Monti et al., 1991; Rodrigues et al., 2013) and has a short lifespan of ca. 2–3 years (Monti et al., 1991; Rodrigues et al., 2013). In southern Brazil, this species attains an average adult size of ca. 30 mm, but larger individuals have previously been reported (e.g. Boehs et al., 2008). In latitudes marked by minimal temperature

variation the reproductive cycle is continuous throughout the year (e.g. Boehs et al., 2008; Luz and Boehs, 2011), but peaks have been recorded in the spring, summer and autumn, with well-defined growth cessation in the winter at mid-latitudes (Barreira and Araujo, 2005; Luz and Boehs, 2011).

2. Material and methods

2.1. Monitoring environmental parameters

Surface temperature (ST, °C), surface salinity (SS, PSU) and $\delta^{18}\text{O}$ of the water ($\delta^{18}\text{O}_w$, V-SMOW) were measured at seasonal and monthly intervals for one year, from August 2008 to August 2009, in several areas of the LLS and in the adjacent open sea (Fig. 1). ST and SS were measured at approximately 10 cm below the water surface using an YSI 556 multiparameter probe. Seasonal and monthly samples of surface water (10 mL) were collected for oxygen isotopic analysis. Seasonal water samples (austral winter, spring, summer and autumn) were taken to establish the $\delta^{18}\text{O}_w$ values of the main sources of freshwater (Tubarão, Duna and Aratingaúba) and seawater input within the LLS, and their relation with SS. Monthly water samples were collected to examine the $\delta^{18}\text{O}_w$ values in areas where living *A. flexuosa* were collected for shell isotope analysis. Daily ST and SS were also recorded every 36 min at the Marine Science Laboratory (Universidade do Sul de Santa Catarina) at the Santo Antônio Lagoon (Fig. 1, n. 15), using the same instrumentation reported above. An Inverse-Distance-Weighting-Method (IDW) was used in ArcGIS to explore spatial variability in SS and $\delta^{18}\text{O}_w$ based on data collected at the seasonal scale. Monthly data on Chlorophyll *a* was obtained from Meurer and Netto (2007), who measured the primary productivity in several locations of the Santo Antônio Lagoon in 2007. Precipitation values for the study area (year 2008–2009) were kindly provided by Epagri/CIRAM (<http://www.inmet.gov.br/portal/>). Astronomic tidal oscillations for Laguna between August 2008 and 2009 were simulated using the free

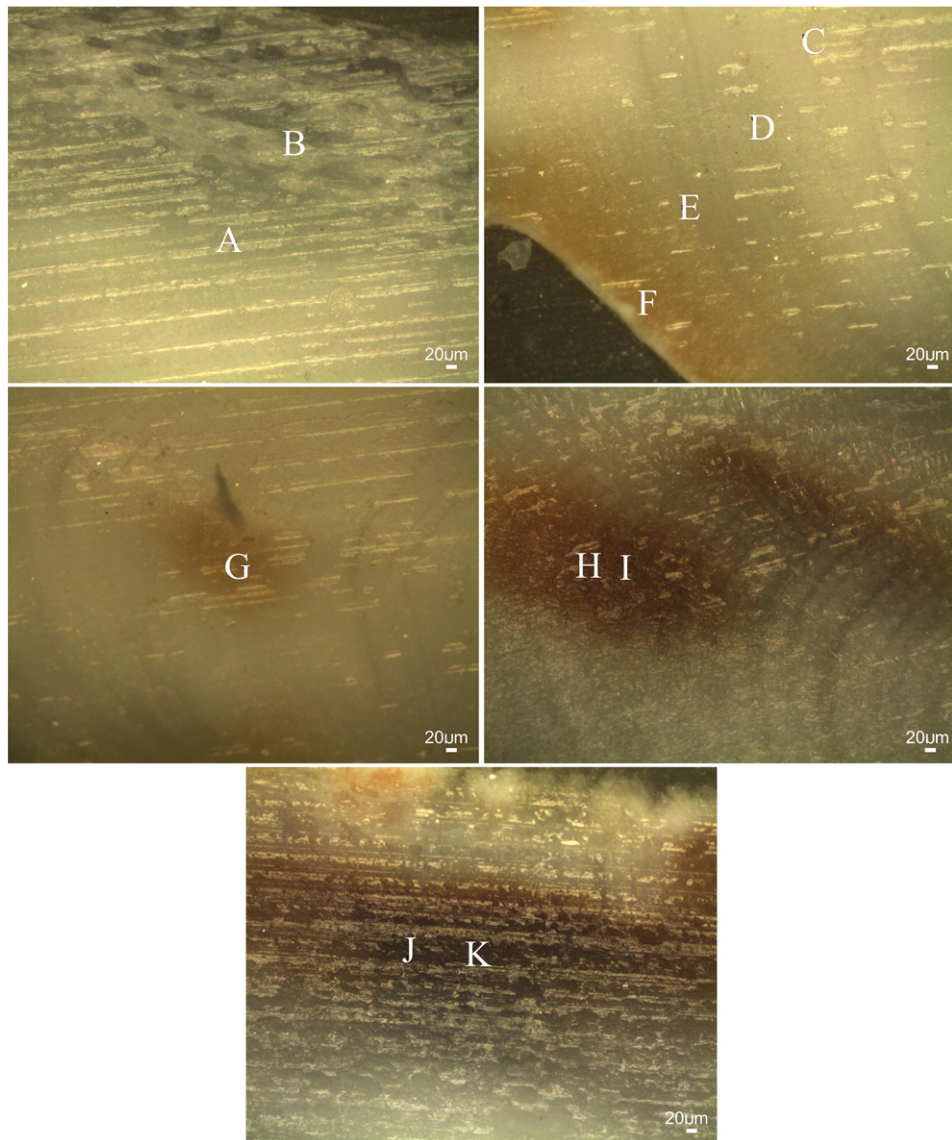


Fig. 3. Optical microscopy images of the internal part of the *Anomalocardia flexuosa* shell (AF-13-2) obtained using a $\times 10$ objective. Regions labelled A–K were investigated using Raman spectroscopy.

software WXTide32 (<http://www.wxtime32.com/>). The tidal simulation does not include weather effects.

2.2. Shell preparation for sclerochronological and stable isotope analyses

From a depth of ca. 50 cm, twelve living specimens of *A. flexuosa* were collected on the 15th of July 2009, from areas 11, 12, 13, 14, and 16 (Fig. 1) of Santo Antônio Lagoon. Immediately after collection the soft parts were removed to prevent the animals from secreting additional shell carbonate. Shell preparation for incremental analysis was performed at the INCREMENTS Research Group of the University of Mainz (Germany). After rinsing and air-drying, the shells were partially embedded in an epoxy resin, then sectioned perpendicularly to the growth lines (from the umbo to the ventral margin; Fig. 2A–C) with a 0.4 mm thick diamond-coated saw blade mounted to a low speed saw (Buehler, IsoMet 1000). From each shell, two slabs of 3 to 5 mm thickness were then cut and glued to a glass slide, ground on glass plates with F800 and F1200 grit SiC powder and polished with 1 μm Al_2O_3 powder. For each shell, one thick-section was used for growth increment analysis, whereas the other was selected for stable isotope analyses. Samples for the analysis of growth increments were immersed in

Mutvei's solution (see Schöne et al., 2005 for details), which gently etches the calcium carbonate while preserving the organic matrix and dyeing the sugars and glycoproteins with Alcian blue. The shell structure of *A. flexuosa* is formed by an outer crossed-lamellar layer (CL) that becomes homogeneous inwards (Taylor et al., 1973). The use of Mutvei's solution in the CL emphasizes the organic-rich growth lines which appear dark blue, whereas the carbonate-rich growth increments appear light blue. This allows shell increments to be easily distinguished by microscopic analysis. Shell slabs were analysed with a Keyence VHX-100 digital microscope at different magnifications (from 300 to 500) in the Department of Archaeology at the University of York. Incremental width was measured in the direction of growth in the outer shell layer (Fig. 2C–E).

Three archaeological shells (CAB1, CAB2, CAB3) were sampled from an archaeological shell mound, Cabeçuda (Fig. 1, n. 12), to compare with data obtained from the modern specimens. The archaeological shells from Cabeçuda were associated with a human burial (Burial 15) dated between 3235 and 3070 calibrated years before present (2σ , AMS, Beta - 383566; Farias and DeBlasis, 2014). The archaeological shells were prepared for stable isotope analysis following the same procedure as the modern specimens.

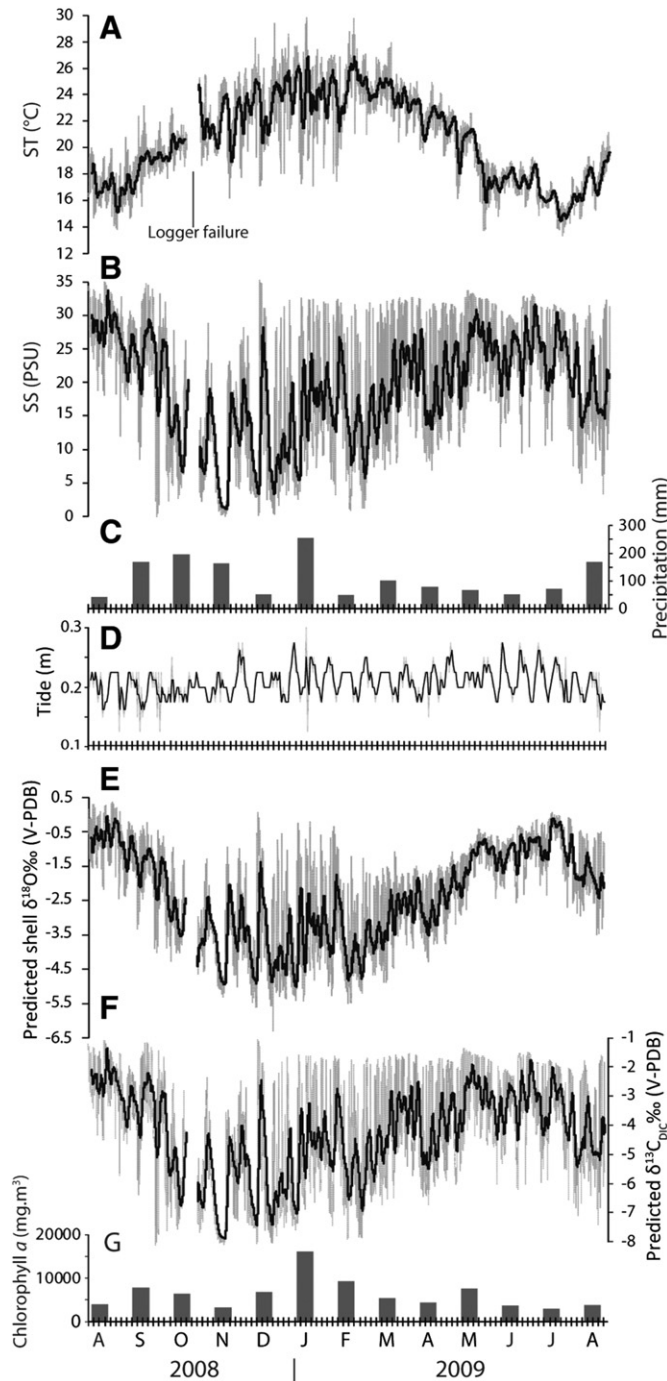


Fig. 4. Environmental information for the southern sector of the LLS, at Santo Antônio Lagoon. A) Daily ST; B) SS; C) monthly total precipitation; D) daily average astronomical tidal oscillation; E) predicted $\delta^{18}\text{O}_w$ values; F) estimated $\delta^{13}\text{C}_{\text{DIC}}$ values; and G) Chlorophyll *a* concentration. (A, B, E, F 205-point moving average; D 2-point moving average).

The shell mineral composition was investigated using X-ray diffraction (XRD), with a mixture of calcite and aragonite standards. Raman spectroscopy was used to increase the accuracy of mineralogical identification of the outer crossed-lamellar layer, as well as to investigate the nature of the pigments that were visible on the section of some specimens. Raman spectra were obtained using an HORIBA XploRA Raman microscope using a $\times 50$ long working distance objective ($\text{NA} = 0.50$) in confocal mode with 532 nm laser wavelength. The shell was sectioned and polished to enable the collection of Raman spectra from the internal shell structure. Eleven positions on the sectioned shell

were analysed with a single spectrum collected in both the pigmented and non-pigmented regions (positions A to K in Fig. 3). Spectra were acquired using LabSpec 5 software set at 3.8 mW laser power at the sample and 1s exposure with each spectrum per region averaged over 40 spectral repetitions. The software package IGOR Pro. 6.32 was used to analyse the Raman spectra using Gaussian peak-fitting procedures.

2.3. Isolating environmentally-controlled growth patterns in modern shells

Shell growth rate decreases as the bivalve grows older. This trend is superimposed by the effect of environmental conditions on the animal's physiology (Schöne, 2008). In order to examine the response of shell growth to environmental change, this age-related trend was removed following the procedure reported in detail in Schöne (2003). In short, after measuring the single increments, the exponential growth function for each shell was estimated, and then a growth index (GI) calculated by dividing the measured value by the estimated growth at each measurement (ratio-based GI). A series of filters (high, low and band pass) were then used to explore low, medium and high frequency signals on growth incremental series (Miyaji et al., 2007; Schöne, 2013). Filters were used with a transition width of 0.02, following Parks-McClellan algorithms in PAST 3.x (Hammer et al., 2001). Spectral analysis of filtered increment time-series was accomplished by means of Continuous Wavelet Transformation (Morlet wavelet, wavenumber 6 <http://paos.colorado.edu/research/wavelets/>) (Torrence and Compo, 1998; Wanamaker et al., 2008). The filtered time-series of each shell was normalized to the global wavelet spectrum, and a 95% confidence interval was applied against a red-noise (autoregressive lag-1) background spectrum.

2.4. Stable isotope analysis

Stable isotope analyses were performed on modern specimens from area 13 (AF-13-1, AF-13-2, AF-13-3) and 12 (AF-12-3), and three archaeological shells (CAB1, CAB2, CAB3). Carbonate samples (ca. 50 to 150 μg) were manually drilled sequentially along the umbo – ventral margin axis from the outer shell layer (Fig. 2B). Samples were taken using a manual microdrill with a 0.4 mm diameter bit. Distances between individual sample spots ranged from 0 to 1.1 mm.

Modern shell oxygen and carbon isotopic composition was measured at the Stable Isotope Facility at the University of Wyoming (USA) using a Thermo Gasbench coupled to a Thermo Delta Plus XL IRMS, after reaction with 99.99% H_3PO_4 (100 μL) at 25 $^\circ\text{C}$ for 24 h. Isotope data were normalized against calibrated NBS19 in-house standards, UWSIF18 ($\delta^{18}\text{O} = -3.3\text{‰}$, $\delta^{13}\text{C} = +2.6\text{‰}$) and UWSIF06 ($\delta^{18}\text{O} = -28.9\text{‰}$, $\delta^{13}\text{C} = +11.6\text{‰}$), with 1σ external reproducibility and average internal precision of 0.2‰ and 0.15‰ for $\delta^{18}\text{O}$ and $\delta^{13}\text{C}$ respectively. Archaeological samples were analysed at the University of Mainz (Germany) on a Thermo Finnigan MAT 253 continuous flow IRMS, coupled to a Gas Bench II, after reaction with 99.99% H_3PO_4 at 72 $^\circ\text{C}$ for 2 h. Isotope data were calibrated against a NBS19 calibrated Carrara marble standard ($\delta^{18}\text{O} = -1.9\text{‰}$, $\delta^{13}\text{C} = +2.0\text{‰}$), with 1σ external reproducibility and internal precision better than 0.06‰ and 0.04‰ for $\delta^{18}\text{O}$ and $\delta^{13}\text{C}$ respectively.

Oxygen isotopic composition of sampled water was analysed via equilibration with CO_2 at the Geochronological Research Center (CPGeo) of the Universidade de São Paulo (Brazil) using a DeltaPlus Advantage (Thermo Finnigan) IRMS. Analytical precision for was better than 0.07‰ for water $\delta^{18}\text{O}$.

Results are reported in δ -notation, and $\delta^{18}\text{O}$ and $\delta^{13}\text{C}$ values are given as parts per mil (‰). Shell $\delta^{18}\text{O}$ and $\delta^{13}\text{C}$ values are reported to V-PDB, whilst water $\delta^{18}\text{O}$ are reported to V-SMOW.

Shell $\delta^{18}\text{O}$ values reflect the temperature and $\delta^{18}\text{O}_w$ values experienced by the animal during shell growth, which is in turn regulated by the animal's physiological tolerance to environmental conditions and endogenous controls (Schöne, 2008). In order to assess the range of

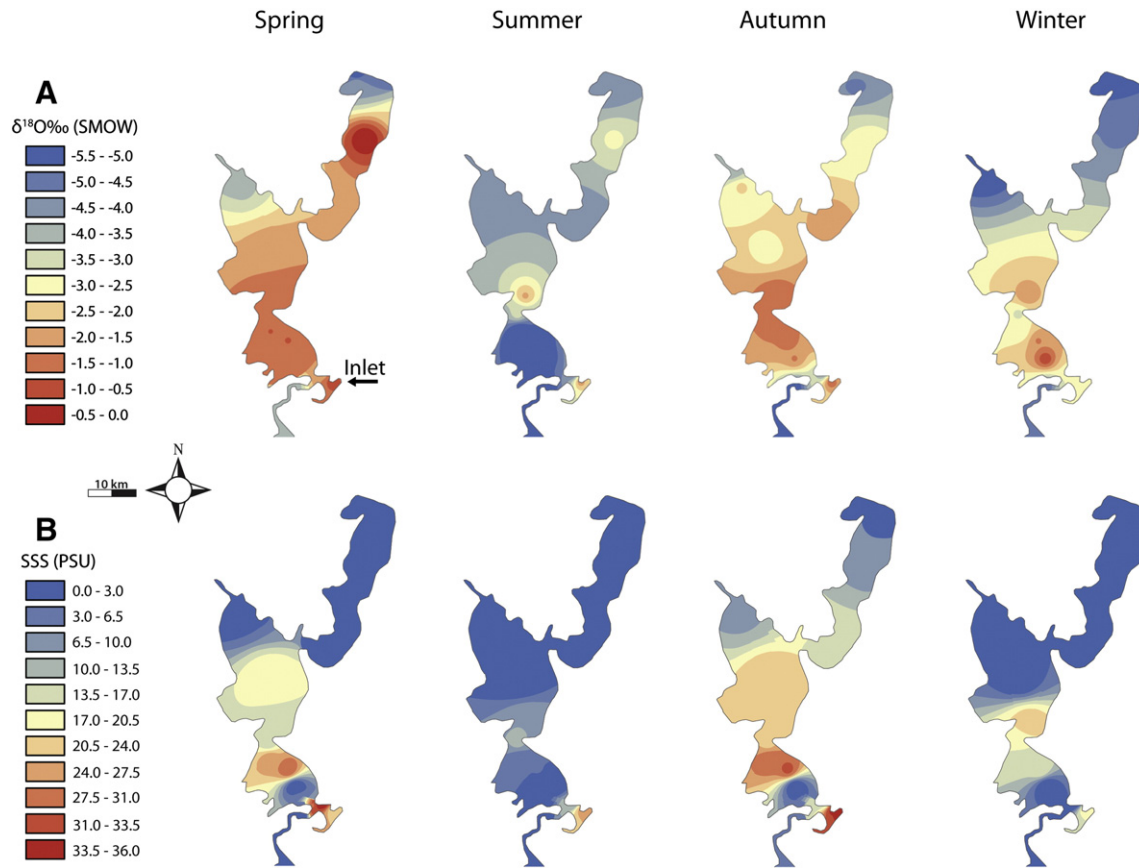


Fig. 5. A) Spatial and seasonal variation in SS and B) $\delta^{18}\text{O}_w$ values for the LLS.

environmental conditions experienced by *A. flexuosa* at the LLS we compared the shell $\delta^{18}\text{O}$ values with highly resolved predicted aragonite $\delta^{18}\text{O}$ values in isotopic equilibrium with instrumentally measured ST and $\delta^{18}\text{O}_w$ values for the study area over one year. We used our locally established $\delta^{18}\text{O}_w$ -SS relationship to derive the $\delta^{18}\text{O}_w$ values from sub-daily SS data. The SS-derived $\delta^{18}\text{O}_w$ values and the measured STs were then used to calculate the shell $\delta^{18}\text{O}$ values according to the empirically derived temperature equation obtained by Grossman and Ku (1986). The equation was slightly modified to convert the $\delta^{18}\text{O}_w$ from V-

SMOW to V-PDB (Dettman et al., 1999):

$$T \text{ (}^\circ\text{C)} = 20.6 - 4.34 \left(\text{shell } \delta^{18}\text{O} - (\delta^{18}\text{O}_w - 0.27) \right) \quad (1)$$

According to this equation, a 1‰ change in shell $\delta^{18}\text{O}$ values corresponds to a change in water temperature of 4.34 °C, providing that the $\delta^{18}\text{O}_w$ remains unchanged. This was not the case for the study area

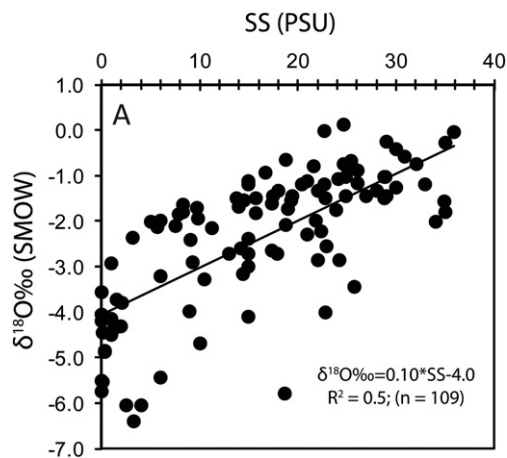


Fig. 6. $\delta^{18}\text{O}_w$ -SS relationship for the LLS over a period of one year.

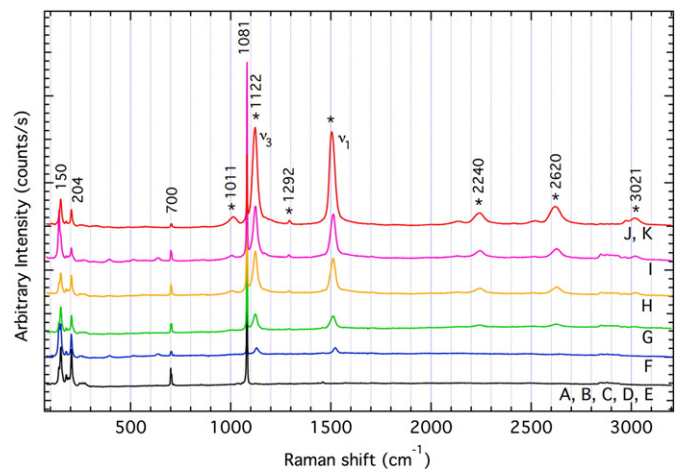


Fig. 7. Raman spectra acquired with 1 cm^{-1} spectral resolution from different regions of specimen AF-13-2 measured at positions A–K in Fig. 3. Peaks denoted with * correspond to the carotenoid signature, while peaks at 150, 204, 700 and 1081 cm^{-1} correspond to the aragonite polymorph of calcium carbonate (as per Urmos et al., 1991). The prominent ν_3 and ν_1 carotenoid peaks are labelled. The ν_1 carotenoid peak shifts to lower wavenumbers as a function of increasing pigmentation.

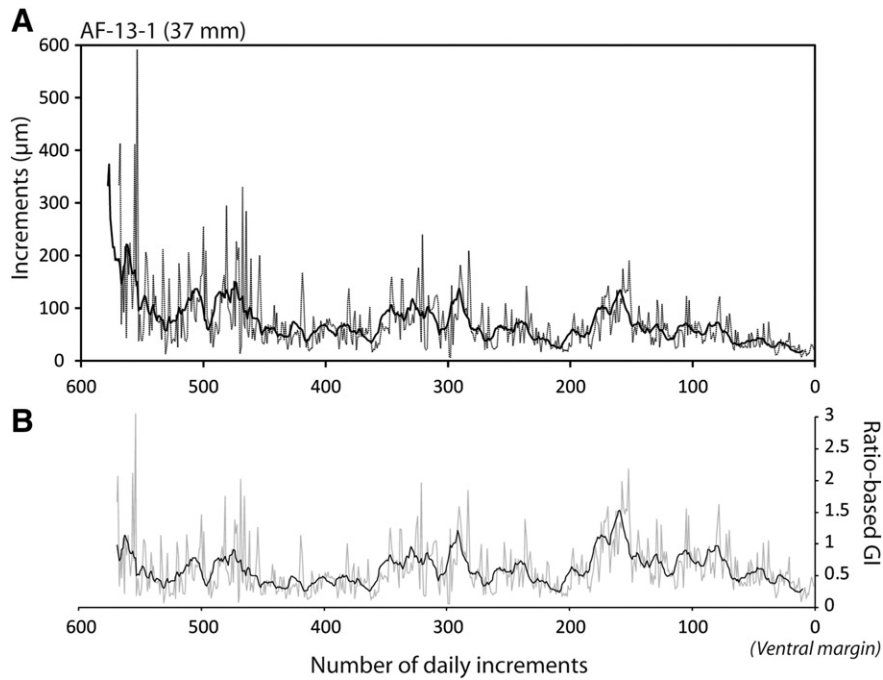


Fig. 8. An example of the growth pattern in *Anomalocardia flexuosa* (specimen AF-13-1). A) Increment width (including 10-points moving average) and B) detrended growth increments using exponential fit (ratio-based GI).

(see below). Coastal areas affected by freshwater input have variable $\delta^{18}\text{O}_w$ values that may complicate palaeotemperature estimations if precise temperature and $\delta^{18}\text{O}_w$ values are not known (e.g. Ingram et al., 1996; Dettman et al., 2004).

The main source of carbon isotopes in bivalve shells is dissolved inorganic carbon (DIC) (e.g. Gillikin et al., 2006; McConnaughey and Gillikin, 2008; Poulain et al., 2010). Compared to seawater, DIC is typically ^{13}C -depleted in lacustrine and estuarine environments due to the larger amount of CO_2 derived from decaying continental organic matter, which often has distinct $\delta^{13}\text{C}$ values (e.g. C3 and C4 plants; O'Leary, 1988), and the dissolution of carbonates (Mook and Tan, 1991). Consequently, freshwater and estuarine molluscs tend to have comparatively lower shell $\delta^{13}\text{C}$ values than their marine counterparts (Dettman et al., 1999; Gillikin et al., 2009). Since the $\delta^{13}\text{C}$ values for the local DIC were not available, we estimated the stable carbon isotope composition for the DIC ($\delta^{13}\text{C}_{\text{DIC}}$) using data collected from Barros et al. (2010) in Babitonga Bay, approximately 200 km north of the study area. The $\delta^{13}\text{C}_{\text{DIC}}$ values from Babitonga Bay are positively correlated with local SS ($R^2 = 0.7$), and represented by the following $\delta^{13}\text{C}_{\text{DIC}}$ -SS relationship:

$$\delta^{13}\text{C}_{\text{DIC}}(\text{‰}) = 0.2 * \text{SS (PSU)} - 8.1 \quad (2)$$

3. Results

3.1. Environmental conditions at Santo Antônio Lagoon

The daily ST from Santo Antônio Lagoon (area 15; Fig. 1) in the southern sector of the LLS show clear seasonal variation (15°C), ranging from 29°C in summer (January–February) to 14°C in winter (July–August) (Fig. 4A). Similarly, the daily SS exhibits a strong seasonal oscillation, ranging from 0 to 35 PSU in spring-summer (October–March) and autumn-winter (May–August), respectively (Fig. 4B). Seasonal changes in SS respond to variations in precipitation over the study area, which was higher in spring-summer compared to autumn-winter (Fig. 4C). High frequency variation in SS and ST values (daily, weekly) instead reflects the effect of mixed semidiurnal tide on the freshwater/seawater

circulation (Fig. 4D). The highest tides facilitate the input of seawater within the LLS, while the opposite occurs with the lowest tides.

The $\delta^{18}\text{O}_w$ values of samples collected at seasonal and monthly intervals ($n = 109$) ranged from $+0.1\text{‰}$ to -6.4‰ . As expected, a clear isotopic gradient was observed from seawater to freshwater endmembers, with average values ranging from $-0.9 \pm 0.9\text{‰}$ in seawater ($n = 4$), to $-3.7 \pm 0.7\text{‰}$ in the Duna River ($n = 4$), $-4.4 \pm 0.9\text{‰}$ in the Aragatingaúba River ($n = 4$), and $-5.0 \pm 0.9\text{‰}$ in the Tubarão River ($n = 4$). Whilst a significant statistical difference was observed for the average $\delta^{18}\text{O}_w$ values between seawater and freshwater ($p < 0.001$, $F = 12.36$, One-way ANOVA), no differences were observed between the rivers ($p < 0.578$, $F = 0.58$). However, the $\delta^{18}\text{O}_w$ values also changed at the seasonal scale (by 6.5‰). Higher and lower $\delta^{18}\text{O}_w$ values were recorded in winter-early spring (August–September) and summer-early autumn (February–April), respectively, tracking generally the salinity distribution (Fig. 5A–B). The $\delta^{18}\text{O}_w$ values showed a moderately positive correlation with the SS values within the LLS (Fig. 6):

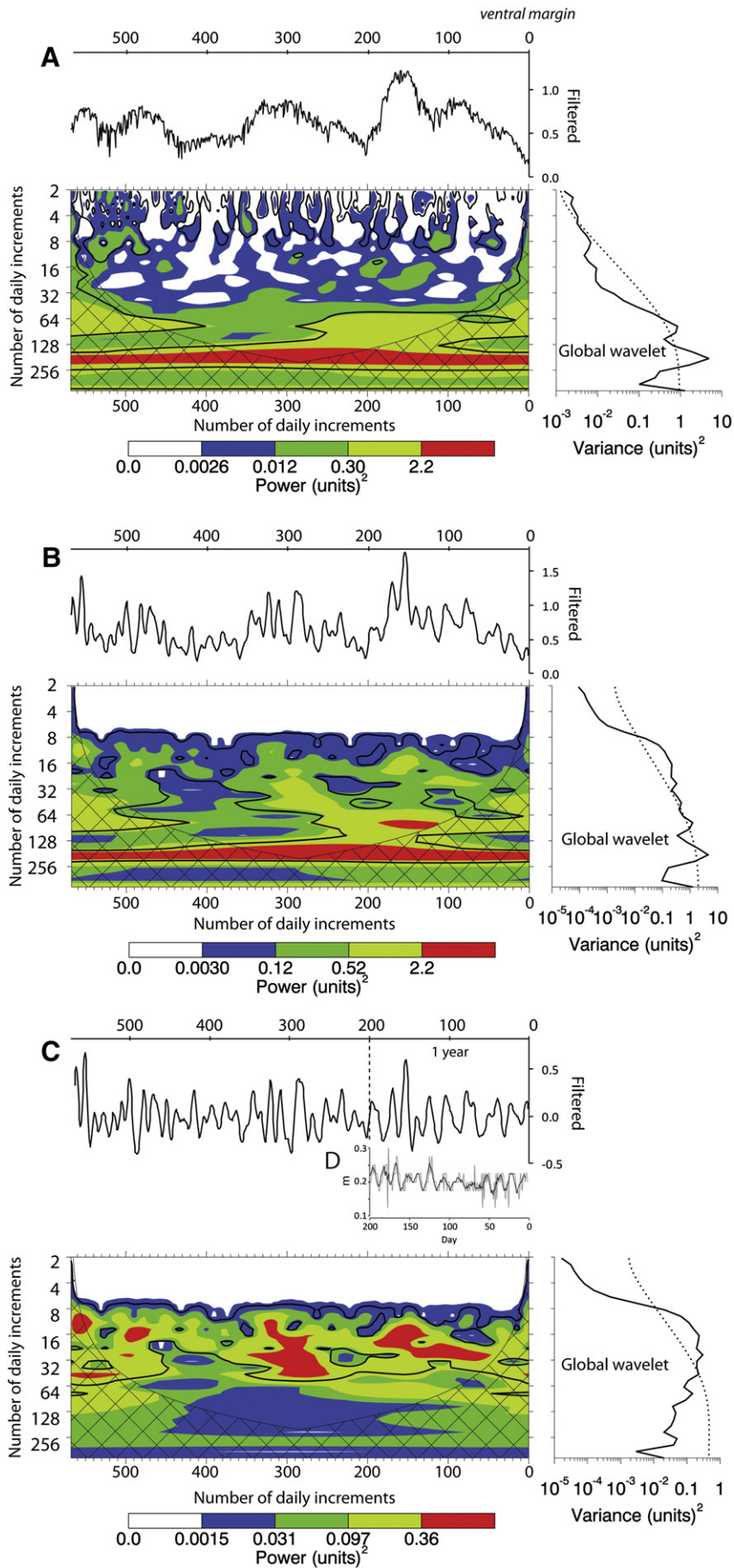
$$\delta^{18}\text{O}_w(\text{‰}) = 0.10 * \text{SS (PSU)} - 4.0 \quad (3)$$

$$R^2 = 0.5; p < 0.001$$

As a result of the seasonal variation in ST and $\delta^{18}\text{O}_w$, the predicted shell $\delta^{18}\text{O}$ values (Fig. 4E) showed a quasi-sinusoidal trend, ranging from $+0.4\text{‰}$ to -6.3‰ in winter and spring-summer respectively, with an annual average value of $-2.3 \pm 1.4\text{‰}$. A similar seasonal trend was observed for the estimated $\delta^{13}\text{C}_{\text{DIC}}$, with lower (-8.1‰) and higher (-1.1‰) values in spring-summer and autumn-winter respectively (Fig. 4F). Chlorophyll *a* showed seasonal variations with higher values in summer (ca. $20,000 \text{ mg/m}^3$) and lower concentrations in autumn and winter (ca. 4000 mg/m^3) (Fig. 4G).

3.2. Mineral and organic composition of the outer shell layer

Both Raman spectroscopy and X-ray diffraction (not shown) indicate that shell of *A. flexuosa* is made of aragonite. The aragonite signature was identified in the Raman spectra by comparing the peak positions at $150, 204, 700$ and 1081 cm^{-1} (the latter being the main carbonate ν_1 band) to other literature (e.g. Urmos et al., 1991). Raman



spectroscopy also revealed that pigmented regions in the outer shell layer of the sampled specimen were carotenoids (Fig. 7). The two prominent peaks in the carotenoid signature, ν_3 and ν_1 , are related to the in-phase stretching of the double and single carbon-carbon bonds in the main polyene chain, respectively (Withnall et al., 2003). The peak intensity of the ν_3 and ν_1 bands increases, with the ν_1 peak position shifting to lower wave numbers as a function of the increasing (i.e., deepening) pigmentation (Fig. 7).

The peak position of the ν_1 Raman band is related to the number of conjugated double bonds in the main polyene chain of the carotenoid and can be used to identify the type of carotenoid in the shell (Withnall et al., 2003). In the case of the *A. flexuosa* shell, two types of carotenoids were identified; β -carotene and decapreno- β -carotene. Carotenoids are commonly found in marine organisms (Urmos et al., 1991; Withnall et al., 2003; Maoka, 2011). Since they are not synthesized *de novo* by animals their presence can be associated with their accumulation through the food (microalgae) (Maoka, 2011).

3.3. Shell growth increments of modern *Anomalocardia flexuosa*

The number of microgrowth lines observed in the outer layer of twelve cross-sectioned specimens of *A. flexuosa* from Santo Antônio Lagoon ranged from 393 to 690, and showed cyclical variations (Fig. 8A–B). The lines were oriented parallel to the direction of shell growth, and separated highly variable microgrowth increments, with widths ranging from 1.3 to 590 μm (average $60.5 \pm 46.8 \mu\text{m}$). The broadest increments were represented in the earliest portion of the shells (e.g. up to 590 μm in AF-13-1; Fig. 8A) and decreased with the ontogenetic age toward the shell ventral margin (from 6.3 to 239 μm).

The age-detrended profile of shell growth increments allowed for a better appreciation of the variation in growth rate as a function of environmental conditions (Fig. 8B). An overall decrease in the growth rate was observed toward the ventral margin of specimen AF-13-1, which represents the last period of shell development prior to live collection in winter 2009. The same pattern was recorded in all the specimens. Reduced growth rate thus seems to correspond with low temperatures as well as low primary productivity. By contrast, an overall increase in shell growth rate was observed in almost all the specimens (91%) before the decreasing trend in winter. The maximum growth rate corresponded with high temperatures and occurred at the time of maximum primary productivity in spring-summer.

The age-detrended growth increments showed distinct periodic cycles. High and low pass filters revealed significant periodicity of ca. 200 microincrements, which likely corresponds to the annual growth period of 200 days (Fig. 9A–B). The low pass filter also revealed bundles with ca. 16 to 32 increments that are significantly detected (red noise at 95% confidence level) with a band pass filter (Fig. 9C). Bundles with ca. 32 increments could correspond with higher astronomical neap tides observed three times a year with a frequency of ca. 32 days. Bundles with ca. 16–14 increments were observed in all the specimens and likely correspond to spring tide-to-spring-tide-cycle (apogee) and/or full-moon-to-new-moon-cycle (perigee) (Schöne and Surge, 2012). The tidal growth pattern was further corroborated by the alignment between the last 200 daily increments and the daily average tidal variation of 200 days prior to shell collection in winter 2009 (Fig. 9D). Tidal growth patterns could be also distinguished by the periodic occurrence of broad, closely spaced daily growth lines during neap and spring tides, and were particularly visible in the juvenile portion of the shell (see also Fig. 2C–E). Similar results have been reported for other species from

tide-controlled settings (Kanazawa and Sato, 2008; Lutz and Rhoads, 1977; Milano et al., 2017; Schöne and Surge, 2012).

3.4. Shell stable isotope composition of modern *Anomalocardia flexuosa*

Modern shells from Santo Antônio Lagoon had average $\delta^{18}\text{O}$ and $\delta^{13}\text{C}$ values ranging from $-1.6 \pm 0.4\text{‰}$ (AF-12-3) to $-2.2 \pm 0.7\text{‰}$ (AF-13-3) and $-0.9 \pm 0.6\text{‰}$ (AF-12-3) to $0.0 \pm 0.7\text{‰}$ (AF-13-1), respectively. Intra-shell $\delta^{18}\text{O}$ variability was highly variable among specimens (from 1.2‰ to 3.3‰ in AF-12-3 and AF-13-1, respectively) and showed cyclical variations representing up to three cycles (e.g. AF-13-2). A similar pattern was roughly displayed by intra-shell $\delta^{13}\text{C}$ values (from 1.9‰ to 2.9‰ in AF-13-2 and AF-13-3, respectively) (Fig. 10A–D).

In conjunction with the sampling resolution and shell incremental record, the isotope cycles enabled us to estimate the life span of analysed specimens and the shell growth rate through ontogeny. The life span of the modern specimens did not exceed 2–3 years, with an average growth rate of $14.2 \pm 4.9 \text{ mm/year}$. *A. flexuosa* grows faster in its first year of shell formation ($19.2 \pm 3.0 \text{ mm/year}$), decreasing in subsequent years ($12.4 \pm 0.7 \text{ mm/year}$), with a minimum rate achieved in the last year of life ($8.2 \pm 3.2 \text{ mm/year}$).

Based on the predicted shell $\delta^{18}\text{O}$ and $\delta^{13}\text{C}_{\text{DIC}}$ values, low and high $\delta^{18}\text{O}$ and $\delta^{13}\text{C}$ values in modern specimens corresponded with warmer/wet (spring-summer) and colder/dry (winter) conditions. This was further corroborated by moderately positive correlations between shell $\delta^{18}\text{O}$ and $\delta^{13}\text{C}$ values for most of the specimens ($R^2 = 0.3$, $p < 0.05$), except for specimen AF-12-3 ($R^2 = 0.01$, $p = 0.696$). However the maximum measured intra-shell $\delta^{18}\text{O}$ range (i.e. 3.3‰, AF-13-1) was considerably lower than the predicted annual range of $\delta^{18}\text{O}$ values (6.7‰). The lowest measured $\delta^{18}\text{O}$ value (-4.2‰ , AF-13-3) was higher by ca. 2.0‰ compared to the lowest predicted counterpart (-6.3‰). An offset of ca. 0.2‰ was also observed between the highest measured ($+0.2\text{‰}$, AF-13-1) and predicted ($+0.4\text{‰}$) $\delta^{18}\text{O}$ values in winter. A temporal alignment between predicted and measured shell $\delta^{18}\text{O}$ values for the last year of shell formation in four specimens illustrated the magnitude of these offsets. Measured shell $\delta^{18}\text{O}$ values were higher by 1.9‰ compared to the minimum predicted average values for spring-summer and lower by 1‰ compared to the maximum average predicted values for winter (Fig. 11). Computing spring-summer offsets into the palaeotemperature equation, we estimated that *A. flexuosa* slowed growth, or stopped it, when average salinity dropped below 15.4 PSU and temperature rose above 22.4 °C. Given the tolerance *A. flexuosa* to salinity values up to 42 PSU (Leonel et al., 1983), slowed growth/growth interruption in winter would most likely be a function of thermal tolerance. The winter offset revealed that *A. flexuosa* slowed the growth, or stopped it, at temperatures below 18.4 °C. As such, the correlation between measured and the average predicted shell $\delta^{18}\text{O}$ values for the last year of growth of all the specimens was moderately weak ($R^2 = 0.3$, $p < 0.001$).

3.5. Archaeological shells

Archaeological specimens had average shell $\delta^{18}\text{O}$ and $\delta^{13}\text{C}$ values ranging from $-1.4 \pm 0.6\text{‰}$ (CAB2) to $-1.7 \pm 0.5\text{‰}$ (CAB2 and CAB3) and $+0.8 \pm 0.5\text{‰}$ (CAB3) to $+0.9 \pm 0.4\text{‰}$ (CAB1), respectively (Fig. 12). Intra-shell $\delta^{18}\text{O}$ variability was very similar among specimens (from 2‰ to 2.5‰ in CAB1 and CAB3 respectively) and showed up to three complete cyclical oscillations (e.g. CBA3). This pattern was roughly displayed by the intra-shell $\delta^{13}\text{C}$ variability (from 1.9‰ to 2.2‰ in CAB1 and CAB3, respectively), which in turn correlated moderately

Fig. 9. Filtered detrended time series using A) high pass, B) low pass and C) band pass filters. D) Alignment between band pass filtered data and average daily tidal oscillation (8-points moving average) for the last 200 days before shell collection. The filtered data is accompanied by the wavelet power spectrum of detrended microgrowth increments. The power in the wavelet power spectrum has been scaled by the global wavelet spectrum. The cross-hatched region is the cone of influence, where zero padding has reduced the variance. Black contour is the 95% significance level, using a red-noise (autoregressive lag1) background spectrum.

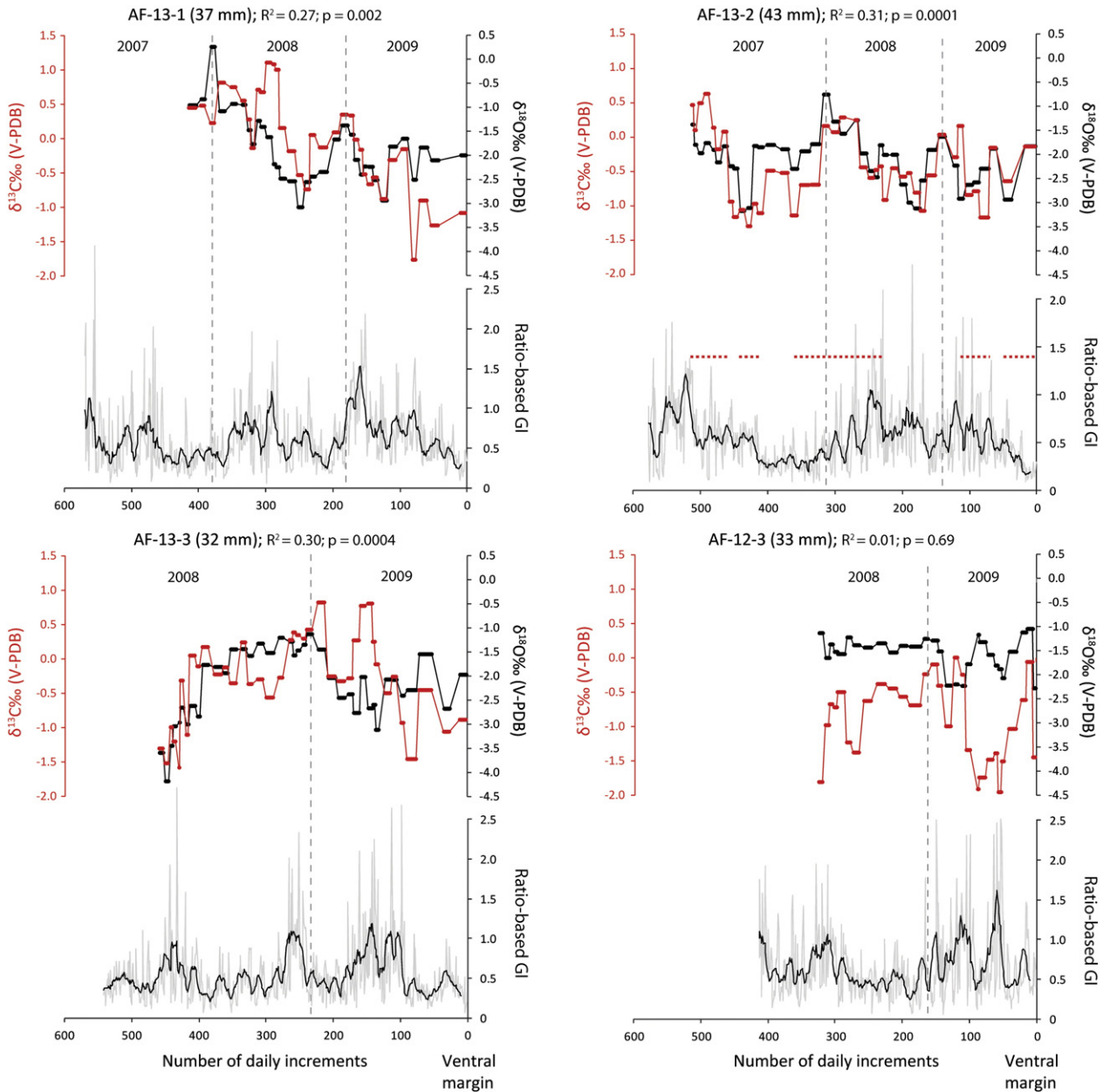


Fig. 10. Shell $\delta^{18}\text{O}$ and $\delta^{13}\text{C}$ values (2-point moving average) and detrended shell growth increments (10-point moving average) of modern *Anomalocardia flexuosa*. The vertical dotted lines represent the ontogenetic years. The red dotted line in specimen AF-13-2 marks the visible traces of carotenoids.

with $\delta^{18}\text{O}$ (from $R^2 = 0.3$ to 0.4 , $p < 0.001$), except for specimen CAB3 ($R^2 = 0.01$, $p = 0.122$). Similar to the modern specimens, the shell growth rate in late Holocene specimens was largely influenced by seasonal temperature/salinity conditions. This was well evidenced by the correspondence between growth cessation (marked by pronounced external growth checks) and peaks of higher shell $\delta^{18}\text{O}$ and $\delta^{13}\text{C}$ values in the specimen CAB3.

Based on winter $\delta^{18}\text{O}$ peaks (e.g. Fig. 12, CAB3), estimated annual growth rates ranged from a minimum of 11.8 ± 4.8 mm/year in the first year (only partially represented in CAB1 and CAB3) to 6.4 ± 1.7 mm/year and 4.4 mm/year (only in CAB3) in the second and third year respectively.

4. Discussion

Similar to other choked lagoons (Kjerfve, 1994), water circulation at the LLS is driven by the complex interaction between winds, tidal

oscillation and seasonal runoff. During the summer, for example, the prevailing NE winds facilitate the movement of less saline water masses toward the southern margins of the lagoon, consequently reducing salinity in Santo Antônio Lagoon. In winter, by contrast, S-SE winds increase the input of seawater into Santo Antônio Lagoon, thus enhancing salinity in the area (Fonseca and Netto, 2006). The high frequency of precipitation in spring-summer compared to winter also contributes to the seasonality of SS in Santo Antônio Lagoon. Santo Antônio Lagoon's $\delta^{18}\text{O}_w$ values are thus expected to reflect the hydrological balance between freshwater and seawater input. The moderate positive correlation between $\delta^{18}\text{O}_w$ and SS values ($R^2 = 0.5$), however, reveals that no simple relationship exists between $\delta^{18}\text{O}_w$ and SS values within the LLS. The moderate correlation can be to some extent explained with changes in seasonal atmospheric circulation, which largely affect the oxygen isotopic composition of precipitations in spring-summer and winter. In late summer and early autumn the region is affected by the South American Summer Monsoon (Carvalho et al., 2004; Raia and Cavalcanti,

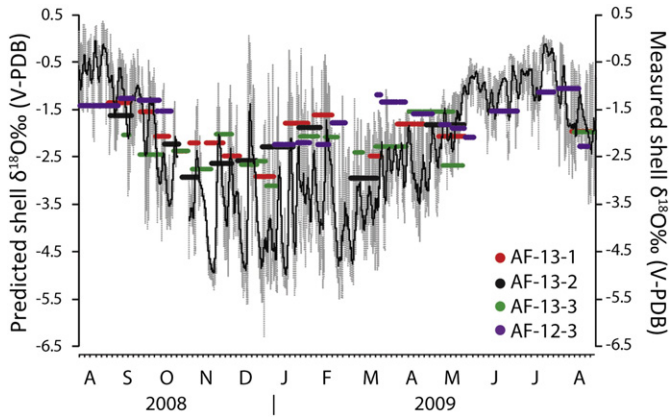


Fig. 11. Temporal alignment between measured and predicted (250-point moving average) shell $\delta^{18}\text{O}$ values for the last year of shell formation (years 2008–2009) in four specimens. The shell $\delta^{18}\text{O}$ values were arranged so that they match the predicted values as closely as possible.

2008), which transports moisture sourced from the Amazon basin, a few thousand kilometres northwest. This atmospheric circulation delivers precipitation which is considerably ^{18}O -depleted (ca. -7%) compared to winter rainfall (ca. -3%) (Cruz et al., 2005a, 2005b; Bernal et al., 2016). During the winter and early spring the region receives a larger cold-dry air mass from the mid latitude South Atlantic Ocean, and heavier precipitations are formed from moisture advected from the nearby Atlantic Ocean (Cruz et al., 2005a; Vera et al., 2002). The average $\delta^{18}\text{O}$ value of the precipitations (ca. -5%) is very close to the average $\delta^{18}\text{O}_W$ value of the rivers analysed in this study ($-4.4 \pm 0.6\%$). The concomitance of summer freshwater input and rainfall isotopic composition was indeed recorded in February 2009 at Santo Antônio Lagoon; the surface water had the minimum SS (3.0 PSU) and $\delta^{18}\text{O}_W$ values (-6.4%), close to those of Tubarão River (2.5 PSU, -6.0%) (Fig. 5A–B). These results thus confirm that the $\delta^{18}\text{O}_W$ values at LLS are

controlled predominantly by the seasonal seawater/freshwater balance, along with the effect of seasonal atmospheric circulation on precipitation $\delta^{18}\text{O}$ values. The $\delta^{18}\text{O}_W$ -SS relationship for the LLS is also expected to be affected by other interplaying factors, such as evaporation and the catchment areas of the rivers (e.g. Lécuyer et al., 2012; Mohan and Walther, 2014), but this is probably minor compared to the mechanisms described above. The effect of the mixed semidiurnal tide is evident on both ST and SS profiles, from daily to monthly timescales. Similarly the estimated $\delta^{13}\text{C}_{\text{DIC}}$ values strongly vary as a function of seasonal changes in seawater and freshwater input.

4.1. Shell increments and stable isotope composition of modern *Anomalocardia flexuosa*

Major variations in growth increment numbers of *A. flexuosa* confirmed that the modern specimens had life spans of ca. 2 to 3 years (ca. 200 days/growing season), in agreement with previous observations along the Brazilian coast (Rodrigues et al., 2013). *A. flexuosa* grows fast during its first year and decreases the rate through ontogeny. As a consequence the isotopic resolution also decreases in the last years of shell growth. As discussed for other bivalve species (Goodwin et al., 2003), the broadest range of environmental conditions experienced by *A. flexuosa* are better expressed in the earliest years of shell development.

Age-detrended increments, $\delta^{18}\text{O}$ and $\delta^{13}\text{C}$ values of shells of *A. flexuosa* appear to respond to interplaying environmental factors. In general, higher growth rate and lower $\delta^{18}\text{O}$ and $\delta^{13}\text{C}$ values correspond to warmer/wet conditions in spring-summer, whereas lower growth rate and higher $\delta^{18}\text{O}$ and $\delta^{13}\text{C}$ values can be associated to colder/dry conditions in winter. Visible peaks relating to carotenoids along the shell of some specimens (e.g. Fig. 10) predominantly correspond with periods of fast growth, and could be indicative of increased metabolic activity. The occurrence of carotenoids is not apparently associated with changes in shell $\delta^{13}\text{C}$ values, and this confirm that variations in shell $\delta^{13}\text{C}$ values are mainly driven by changes in $\delta^{13}\text{C}_{\text{DIC}}$. However

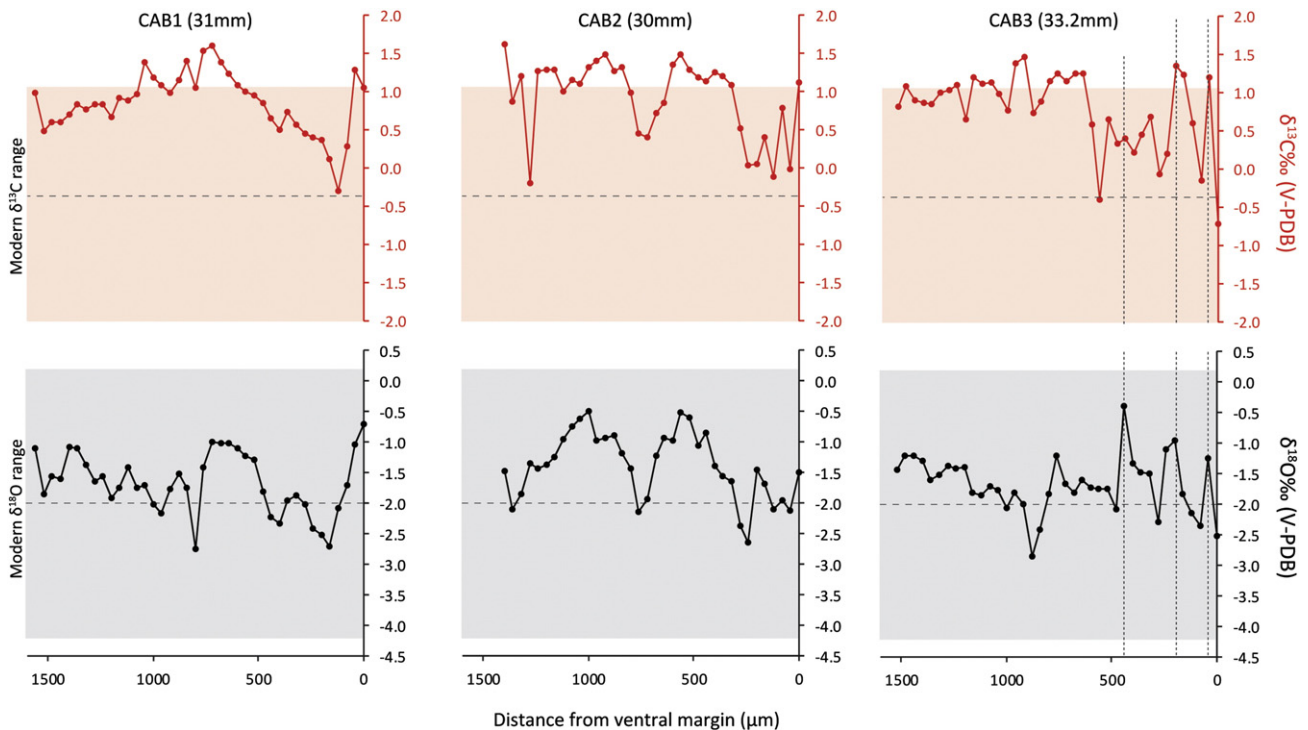


Fig. 12. Shell $\delta^{18}\text{O}$ and $\delta^{13}\text{C}$ values of late Holocene archaeological specimens from Cabeçuda shell mound. The vertical dotted lines in CAB3 mark the external growth checks observed only on this specimen. The red and grey bands represent the $\delta^{13}\text{C}$ and $\delta^{18}\text{O}$ ranges, respectively, observed in modern specimens.

carotenoids are also accumulated in animal gonads and are thought to be crucial for reproduction (Maoka, 2011). Visible concentrations of carotenoids might thus correspond with peaks in the reproductive cycle. Further studies are required to test this hypothesis.

Despite this general pattern, no significant correlations were found between average growth increments and their isotopic signatures for both $\delta^{18}\text{O}$ ($R^2 = 0.00$ to 0.08 , $p = 0.92$ to 0.07) and $\delta^{13}\text{C}$ ($R^2 = 0.11$ to 0.00 , $p = 0.05$ to 0.82) values. The lack of significant correlations probably arises from variations in sample resolution, environmental stress and endogenous mechanisms (e.g. Goodwin et al., 2003). The isotopic resolution in this study ranged from 7 ± 2.6 (AF-13-1) to 9 ± 3.6 (AF-12-3) days, decreasing in winter and near the shell ventral margin (up to ca. 20 days), while increasing during favourable conditions in spring-summer and in the juvenile portion of the shell (up to ca. 1 day).

Despite the increased growth rate of *A. flexuosa* during spring-summer compared to winter, shell $\delta^{18}\text{O}$ values did not record the full range of temperature and salinity conditions in spring-summer. This was confirmed by episodes of reduced growth rate between peaks of maximum growth rates in spring-summer (Fig. 8A–B). Slowed growth, or growth cessation, in spring-summer most likely reflects the response of *A. flexuosa* to increased freshwater circulation and decreased salinity values below its physiological tolerance. According to previous studies, *A. flexuosa* tolerates waters with salinity conditions ranging between 17 and 42 PSU (Leonel et al., 1983; Monti et al., 1991; Silva-Cavalcanti and Costa, 2011; Rodrigues et al., 2013), while at Santo Antônio Lagoon the average values were considerably lower in spring-summer (ca. 5 to 10 PSU), notably from October to January (Fig. 4B). As a consequence, *A. flexuosa* reduce/stop growth for days or weeks during periods of minimum salinity (< 15 PSU). Furthermore, seawater circulation is reduced and salinity values drop considerably during low tide, particularly during spring-summer. It is thus likely that in warmer/wet months *A. flexuosa* remains active predominantly during the highest tides, when salinity reaches the highest values.

Growth cessation may also reflect the impact of sedimentation rate (Monti et al., 1991; Rodrigues et al., 2013), which increases in the study area in summer (Fonseca and Netto, 2006), and is known to affect molluscs in estuarine and coastal areas (Anderson, 2008; Norkko et al., 2002; Peterson, 1985). Aside from these major environmental factors, growth interruption in spring-summer might be also associated with spawning intervals (Schöne et al., 2005; Kanazawa and Sato, 2008), observed in *A. flexuosa* during spring, summer and autumn in southern Brazilian coast (Barreira and Araujo, 2005; Luz and Boehs, 2011).

Our study indicates that *A. flexuosa* from Santo Antônio Lagoon attain the maximum and minimum growth rates in spring-summer and winter respectively, as a response to seasonal temperatures and possibly also nutrient availability. Shell $\delta^{18}\text{O}$ values record both temperature and salinity variations, thus is a suitable candidate for palaeoenvironmental reconstructions. However, the duration and rate of shell growth is strongly affected by changes in freshwater circulation and salinity. Therefore shell $\delta^{18}\text{O}$ values of *A. flexuosa* may not be a suitable proxy for assessing large variations in freshwater-seawater balance in the past, as the animal will stop recording these conditions below its salinity tolerance (ca. 15 PSU). The moderate positive correlations between shell $\delta^{18}\text{O}$ and $\delta^{13}\text{C}$ values indicate that shell stable carbon isotope composition is driven mainly by seasonal variations in $\delta^{13}\text{C}_{\text{DIC}}$, and thus is a promising proxy for salinity variations.

4.2. Archaeological shells

The isotopic profiles from the archaeological shells associated with the human burial dated to 3 ka cal BP show some interesting differences compared to the modern counterparts. Whilst the average shell $\delta^{18}\text{O}$ values were fairly comparable, archaeological specimens showed a much narrower intra-shell $\delta^{18}\text{O}$ variability compared to the modern

ones (Fig. 12). By contrast the average shell $\delta^{13}\text{C}$ values were higher in late Holocene specimens by ca. 1.3‰ compared to the modern shells. Their intra-shell $\delta^{13}\text{C}$ range was also less variable and narrower than in modern specimens.

These isotopic differences likely reflect changes in water temperature and hydrological balance between the late Holocene and present day at the LLS, although the magnitude of these changes remains complex to estimate. For example, we have demonstrated that both temperature and $\delta^{18}\text{O}_{\text{w}}$ values display strong seasonal variations in the LLS, and were both simultaneously responsible for intra-annual shell $\delta^{18}\text{O}$ variability in modern specimens. Intra-annual ST and $\delta^{18}\text{O}_{\text{w}}$ values are unknown for the past, and as such, the application of palaeotemperature equations on fossil shells from estuarine environments are greatly limited (Ingram et al., 1996).

Despite these limitations, the lower variability in intra-shell $\delta^{18}\text{O}$ and $\delta^{13}\text{C}$ values may reflect a reduced seasonality in water temperature and/or salinity during the late Holocene compared to the present day. It is worth noting that several lines of evidence indicate a general sea-level highstand along the southern coast of Brazil during the middle Holocene, followed by a drop to the present day level (Angulo et al., 1999, 2006). Recent geomorphological and sedimentary analyses reveal that during the early Holocene the LLS, and surrounding areas, were submerged by the effect of post-glacial sea-level rise, forming a large bay. At that time, the delta of the Tubarão River was retracted further inland, toward the Serra do Tabuleiro. This palaeobay was subject to direct oceanic circulation. A change from this transgressive open-marine embayment to a coastal lagoon occurred about 6 ka cal BP, due to the achievement of a balance between sea-level rise and sedimentary supply, and the consequent formation of a sand barrier to the south of Entrada da Barra inlet. Subsequently, the Tubarão river delta silted up most of this bay-lagoon and the river inflow gradually advanced in Santo Antônio Lagoon until reaching its current configuration (Giannini et al., 2010; Fornari et al., 2012). The intra-shell $\delta^{18}\text{O}$ and $\delta^{13}\text{C}$ values discussed in the present study would corroborate these palaeoenvironmental reconstructions. Archaeological shell isotope data indirectly indicate a reduced seasonal freshwater-seawater balance at ca. 3 ka cal BP, which agrees reasonably with the increased marine circulation. Modern shells instead show a higher seasonal variability in freshwater-seawater balance due to the modern configuration of the LLS.

An additional factor that could have promoted the lower amplitudes of intra-shell $\delta^{18}\text{O}$ values may have been a reduction in precipitation and/or changes in $\delta^{18}\text{O}$ values of precipitations. While the former could have an indirect effect on the $\delta^{13}\text{C}$ by increasing $\delta^{13}\text{C}_{\text{DIC}}$ values, the latter would not explain the reduced amplitude of intra-shell $\delta^{13}\text{C}$ values. Furthermore palaeoclimate reconstructions based on speleothem $\delta^{18}\text{O}$ values and Sr/Ca ratios from southern Brazil point to an intense activity of the South American Monsoon System during the late Holocene. This atmospheric system is the dominant precipitation regime in southern Brazil and is responsible for the strong seasonal variation in rainfall $\delta^{18}\text{O}$ values over the region (Cruz et al., 2005a, 2005b; Bernal et al., 2016). Thus the most likely explanation is that covariation in shell $\delta^{18}\text{O}$ and $\delta^{13}\text{C}$ values and their reduced seasonal amplitude reflect a reduced seasonal seawater-freshwater balance, and enhanced marine exposure.

Other factors might have contributed to the overall decrease of shell $\delta^{13}\text{C}$ values in modern specimens (ca. 1.3‰) compared to those from the late Holocene. In general, a positive shift of 1‰ to 1.5‰ is expected in the $\delta^{13}\text{C}$ values of modern aquatic carbonates due to the increased emission of ^{12}C in the atmosphere by industrial burning of fossil fuels (e.g. Friedli et al., 1986; Sonnerup et al., 1999; Surge et al., 2003). The lower shell $\delta^{13}\text{C}$ values in modern specimens might also reflect a general decrease of $\delta^{13}\text{C}_{\text{DIC}}$ values due to higher nutrient supply and eutrophication of Santo Antônio Lagoon (e.g. Surge et al., 2003). For example, Barros et al. (2010) report the lowest $\delta^{13}\text{C}_{\text{DIC}}$ values in Babitonga Bay in areas that receive heavy loads of untreated domestic sewage. This

might be expected for Tubarão River today as it drains areas affected by the use of pesticides, waste from intensive pig farming, as well as industrial and urban effluents (Osório et al., 2014). Moreover, differing average shell $\delta^{13}\text{C}$ values between archaeological and modern specimens could be associated with changes in vegetation composition and structure in the LLS from the late Holocene. Decaying organic matter derived from plants contributes to defining the $\delta^{13}\text{C}$ values of DIC (Mook and Tan, 1991). Present day vegetation at the LLS includes species found mainly in salt marshes (e.g. *Spartina alterniflora*) and swamps (e.g. *Acrostichum aureum*), together with small patches of mangrove forest (e.g. *Laguncularia racemosa*). However, the LLS marks the present southern limit of the western South Atlantic mangroves, which are replaced southwards by salt marsh vegetation (Schaeffer-Novelli et al., 1990; Soares et al., 2012). *Laguncularia racemosa*, the dominant mangrove vegetation in the LLS, has a local $\delta^{13}\text{C}$ value typical of C3 plants (-26.4%), while local *Spartina alterniflora* from salt marshes has a $\delta^{13}\text{C}$ value consistent with C4 plants (-12.7%) (Tognella et al., 2016). Higher average shell $\delta^{13}\text{C}$ values in archaeological specimens could, to some degree, reflect a higher contribution of salt marsh-derived C4 plant types to dissolved inorganic carbon at 3 cal ka BP compared to present day.

How past populations interacted and responded to coastal and environmental changes at the LLS during the Holocene is still a matter of debate. The sambaqui culture had its maximum expansion during the middle-late Holocene (from 6 to 1.5 ka BP), as attested by the emergence and proliferation of shell mounds, most of which are made of the shells of *A. flexuosa*. In agreement with other palaeoenvironmental records, our results indicate that the builders of Cabeçuda shell mound at ca. 3 ka BP exploited *A. flexuosa* in environments marked by lower salinity variations compared to present day at the LLS. Given the limited tolerance of *A. flexuosa* to low salinity waters, the results could reinforce the hypothesis that the reorganization of coastal environments and increased oceanic exposure created more suitable conditions for *A. flexuosa* in the study area between 6 and 1.5 ka BP, contributing to maintain a long-term cultural practice.

5. Conclusion

The bivalve *Anomalocardia flexuosa* is a widely distributed intertidal and subtidal mollusc in coastal areas of Latin America, from the Caribbean to Uruguay. It is abundant in archaeological and sedimentary records, and constitutes an important economic resource for communities (both past and present) living along the Brazilian coast. Using highly-resolved sclerochronological and stable isotopic analyses, we unlocked relevant biological and environmental information from modern and sub-fossil mollusc shells from the Laguna Estuarine System in southern Brazil. We demonstrated the effect of temperature and salinity on the seasonal growth patterns in modern specimens from this subtropical coastal area of Atlantic South America. The isotopically recorded information in the aragonitic shell carbonate thus can be used to assess past environmental conditions using fossil shells from archaeological and sedimentary records. Sclerochronological information (shell growth patterns and stable isotope) could potentially help assessment and management strategies while revealing the impact of local environmental conditions on modern populations.

Acknowledgments

The authors are grateful to Chandelle Macdonald (University of Wyoming), Maria Helena Bezerra Maia de Hollanda and Alyne Barros (Laboratório de Isótopos Estáveis of the Universidade de São Paulo), Milene Fornari (Universidade Estadual Paulista, Campus São Vicente), Angel Álvarez Larena and Javier Martínez (Servei de Difracció de Raigs X, Universitat Autònoma de Barcelona, Spain), Vera Lúcia da Silva Ranghetti (Epagri/Ciram), Krista McGrath (University of York) and Mark Skinner (Simon Fraser University). All necessary permits were

obtained for the described study, which complied with all relevant regulations of the Instituto do Patrimônio Histórico e Artístico Nacional – IPHAN (protocol no 01510.01513/2012-92, 01510.000956/2013-47) and ICMBio (IMABA, SISBIO) for sampling, exporting and analysing modern shells of *Anomalocardia flexuosa* from the LLS (protocol no 113508). The modern and archaeological shells used in this study are stored at the Department of Archaeology of the University of York (UK). Fig. 1 was produced with data available from the U.S. Geological Survey and NASA Land Processes Distributed Active Archive Center (LP DAAC) Products. This research was funded by the São Paulo Research Foundation (FAPESP) project “Sambaquis e Paisagem” (Ref. 04/11038-0; Brazil), “Evolução da Floresta Atlântica” (Ref. 05/51034-6; Brazil), mobility grant (Ref. PA1002165) from the Spanish National Research Council (Spain). R.A.R.P. is grateful to the Brazilian funding council CNPq for the PhD scholarship provided. The authors are grateful to the comments of the two anonymous reviewers and the editor, which improved the quality of the manuscript.

Appendix A. Supplementary data

Supplementary data to this article can be found online at <http://dx.doi.org/10.1016/j.palaeo.2017.01.006>.

Reference

- Anderson, M.J., 2008. Animal-sediment relationships re-visited: characterising species' distributions along an environmental gradient using canonical analysis and quantile regression splines. *J. Exp. Mar. Biol. Ecol.* 366, 16–27.
- Angulo, R.J., Giannini, P.C.F., Suguio, K., Pessenda, L.C.R., 1999. Relative sea-level changes in the last 5500 years in southern Brazil (Laguna-Imbituba region, Santa Catarina State) based on vermetid ^{14}C ages. *Mar. Geol.* 159, 323–339.
- Angulo, R.J., Lessa, G.C., de Souza, M.C., 2006. A critical review of mid- to late-Holocene sea-level fluctuations on the eastern Brazilian coastline. *Quat. Sci. Rev.* 25, 486–506.
- Aravena, G., Broitman, B., Stenseth, N.C., 2014. Twelve years of change in coastal upwelling along the central-northern coast of Chile: spatially heterogeneous responses to climatic variability. *PLoS One* 9, e90276.
- Baker, P.A., Fritz, S.C., 2015. Nature and causes of quaternary climate variation of tropical South America. *Quat. Sci. Rev.* 124, 31–47.
- Bardach, J.E., 1997. Sustainable Aquaculture. Wiley, USA.
- Barreira, C.A.R., Araujo, M.L.R., 2005. Ciclo reprodutivo de *Anomalocardia brasiliana* (Gmelin, 1791) (Mollusca, Bivalvia, Veneridae) na praia do Canto da Barra, Fortim, Ceará, Brasil. vol. 31. B. Inst. Pesca, São Paulo, pp. 9–20.
- Bastos, M.Q.R., Santos, R.V., Tykot, R.H., Mendonça de Souza, S.M.F., Rodrigues-Carvalho, C., Lessa, A., 2015. Isotopic evidences regarding migration at the archaeological site of Praia da Tapera: new data to an old matter. *J. Archaeol. Sci. Rep.* 4, 588–595.
- Barros, G.V., Martinelli, L.A., Oliveira Novais, T.M., Ometto, J.P.H.B., Zuppi, G.M., 2010. Stable isotopes of bulk organic matter to trace carbon and nitrogen dynamics in an estuarine ecosystem in Babitonga Bay (Santa Catarina, Brazil). *Sci. Total Environ.* 408, 2226–2232.
- Bernal, J.P., Cruz, F.W., Strikis, N.M., Wang, X., Deininger, M., Catunda, M.C.A., Ortega-Obregón, C., Cheng, H., Edwards, R.L., Auler, A.S., 2016. High-resolution Holocene South American monsoon history recorded by a speleothem from Botuverá Cave, Brazil. *Earth Planet. Sci. Lett.* 450, 186–196.
- Boehs, G., Absher, T.M., Cruz-Kaled, A.C., 2008. Ecologia populacional de *Anomalocardia brasiliana* (Gmelin, 1791) (Bivalvia, Veneridae) na Baía de Paranaguá, Paraná, Brasil. 34. Boletim do Instituto de Pesca, pp. 259–270.
- Carré, M., Bentalieb, I., Blamart, D., Ogle, N., Cardenas, F., Zevallos, S., Kalin, R.M., Ortlieb, L., Fontugne, M., 2005. Stable isotopes and sclerochronology of the bivalve *Mesodesma donacium*: potential application to Peruvian paleoceanographic reconstructions. *Palaeogeogr. Palaeoclimatol. Palaeoecol.* 228, 4–25.
- Carvalho do Amaral, P.G., Fonseca Giannini, P.C., Sylvestre, F., Ruiz Pessenda, L.C., 2012. Paleoenvironmental reconstruction of a Late Quaternary lagoon system in southern Brazil (Jaguaruna region, Santa Catarina state) based on multi-proxy analysis. *J. Quat. Sci.* 27, 181–191.
- Carvalho, L.M.V., Jones, C., Liebmann, B., 2004. The South Atlantic convergence zone: intensity, form, persistence, and relationships with intraseasonal to interannual activity and extreme rainfall. *J. Clim.* 17, 88–108.
- Colonese, A.C., Mannino, M.A., Bar-Yosef Mayer, D.E., Fa, D.A., Finlayson, J.C., Lubell, D., Stiner, M.C., 2011. Marine mollusc exploitation in Mediterranean prehistory: an overview. *Quat. Int.* 239, 86–103.
- Colonese, A.C., Collins, M., Lucquin, A., Eustace, M., Hancock, Y., Ponzoni, R.A.R., DeBlasis, P., Figuti, L., Wesolowski, V., Plens, C., Eggers, S., Farias, D., Gledhill, A., Craig, O., 2014. Long-term resilience of late Holocene coastal subsistence system in southeastern South America. *PLoS One* 9 (4), e93854. <http://dx.doi.org/10.1371/journal.pone.0093854>.
- Cruz Jr., F.W., Karmann, I., Viana Jr., O., Burns, S.J., Ferrari, J.A., Vuille, M., Sial, A.N., Moreira, M.Z., 2005a. Stable isotope study of cave percolation waters in subtropical Brazil: implications for paleoclimate inferences from speleothems. *Chem. Geol.* 220, 245–262.

- Cruz Jr., F.W., Burns, S.J., Karmann, I., Sharp, W.D., Vuille, M., Cardoso, A.O., Ferrari, J.A., Dias, P.L.S., Viana Jr., O., 2005b. Insolation driven changes in atmospheric circulation over the past 116,000 years in subtropical Brazil. *Nature* 434, 63–66.
- DeBlasis, P., Fish, S.K., Gaspar, M.D., Fish, P.R., 1998. Some references for the discussion of complexity among the sambaqui moundbuilders from the southern shores of Brazil. *Rev. Arqueol. Am.* 15, 75–105.
- DeBlasis, P., Kneip, A., Scheel-Ybert, R., Giannini, P.C.F., Gaspar, M.D., 2007. Sambaquis e paisagem: dinâmica natural e arqueologia regional no litoral do Sul do Brasil. *Arqueologia Suramericana* 3 (1), 29–61 (ISSN 1794-4780).
- Defeo, O., Castrejón, M., Ortega, L., Kuhn, A.M., Gutiérrez, N.L., Castilla, J.C., 2013. Impacts of climate variability on Latin American small-scale fisheries. *Ecol. Soc.* 18, 1–30.
- Dettman, D.L., Flessa, K.W., Roopnarine, P.D., Schöne, B.R., Goodwin, D.H., 2004. The use of oxygen isotope variation in shells of estuarine mollusks as a quantitative record of seasonal and annual Colorado river discharge. *Geochim. Cosmochim. Acta* 68, 1253–1263.
- Dettman, D.L., Reische, A.K., Lohmann, K.C., 1999. Controls on the stable isotope composition of seasonal growth bands in aragonitic fresh-water bivalves (Unionidae). *Geochim. Cosmochim. Acta* 63, 1049–1057.
- Erlanson, J.M., 2001. The archaeology of aquatic adaptations: paradigms for a new millennium. *J. Archaeol. Res.* 9, 287–350.
- Farias, D.S.E., DeBlasis, P., 2014. Programa de salvamento arqueológico e educação patrimonial na área de duplicação da BR-101 trecho Ponte de Cabeçadas, Laguna/SC. Relatório final de pesquisa, Tubarão, SC.
- Figuti, L., 1993. O homem pré-histórico, o molusco e o sambaqui. *Revista do Museu de Arqueologia e Etnologia USP* 3, 67–80.
- Fonseca, G., Netto, S.A., 2006. Shallow sublittoral benthic communities of the Laguna Estuarine System, South Brazil. *Braz. J. Oceanogr.* 54, 41–54.
- Fornari, M., Giannini, P.C.F., Rodrigues, D., 2012. Facies associations and controls on the evolution from a coastal bay to a lagoon system, Santa Catarina, Brazil. *Mar. Geol.* 323–325, 56–68.
- França, M.C., Cohen, M.C.L., Pessenda, L.C.R., Rossetti, D.F., Lorente, F.L., Buso Junior, A.A., Guimarães, J.T.F., Friaes, Y., Macario, K., 2013. Mangrove vegetation changes on Holocene terraces of the Doce River, southeastern Brazil. *Catena* 110, 59–69.
- Friedli, H., Lotscher, H., Oeschger, H., Siegenthaler, U., Stauffer, B., 1986. Ice core record of the $^{13}\text{C}/^{12}\text{C}$ ratio of atmospheric CO_2 in the past two centuries. *Nature* 324, 237–238.
- Garcia, A.M., Vieira, J.P., Winemiller, K.O., 2003. Effects of 1997–1998 El Niño on the dynamics of the shallow-water fish assemblage of the Patos Lagoon Estuary (Brazil). *Estuar. Coast. Shelf Sci.* 57, 489–500.
- García-March, J.R., Surge, D., Lees, J.M., Kersting, D.K., 2011. Ecological information and water mass properties in the Mediterranean recorded by stable isotope ratios in *Pinna nobilis* shells. *J. Geophys. Res.* 116, G02009.
- Gaspar, M., DeBlasis, P., Fish, S.K., Fish, P.R., 2008. Sambaquis (shell mound) societies of coastal Brazil. In: Silverman, H., Isbell, W. (Eds.), *Handbook of South American Archaeology*. Springer, New York, pp. 319–335.
- Gaspar, M.D., Klokler, D.M., DeBlasis, P., 2011. Traditional fishing, mollusk gathering, and the shell mound builders of Santa Catarina, Brazil. *J. Ethnobiol.* 31, 188–212.
- Giannini, P.C.F., Sawakuchi, A.O., Martinho, C.T., Tatum, S.H., 2007. Eolian depositional episodes controlled by Late Quaternary relative sea level changes on the Laguna-Lambituba coast, South Brazil. *Mar. Geol.* 237 (2007), 143–168.
- Giannini, P.C.F., Villagran, X.S., Fornari, M., Nascimento Junior, D.R., Menezes, P.L., Tanaka, A.P.B., Assunção, D.C., DeBlasis, P., Amaral, P.C., 2010. Interações entre evolução sedimentar e ocupação humana pré-histórica na costa centro-sul de Santa Catarina, Brasil. Interactions between sedimentary evolution and prehistoric human. *Bol. Mus. Para. Emílio Goeldi. Cienc. Hum.* 5, 105–128.
- Gillikin, D.P., Lorrain, A., Bouillon, S., Willenz, P., Dehairs, F., 2006. Stable carbon isotopic composition of *Mytilus edulis* shells: relation to metabolism, salinity, $\delta^{13}\text{C}_{\text{DIC}}$ and phytoplankton. *Org. Geochem.* 37, 1371–1382.
- Gillikin, D.P., Hutchinson, K.A., Kumai, Y., 2009. Ontogenic increase of metabolic carbon in freshwater mussel shells (*Pyganodon cataracta*). *J. Geophys. Res.* 114, G01007.
- Goodwin, D.H., Schöne, B.R., Dettman, D.L., 2003. Resolution and fidelity of oxygen isotopes as paleotemperature proxies in bivalve mollusk shells: models and observations. *PALAIOS* 18, 110–125.
- Grossman, E.L., Ku, T.-L., 1986. Oxygen and carbon isotope fractionation in biogenic aragonite: temperature effects. *Chem. Geol. Isot. Geosci.* 59, 59–74.
- Gyllencreutz, R., Mahiques, M.M., Alves, D.V.P., Wainer, I.K.C., 2010. Mid- to late-Holocene paleoceanographic changes on the southeastern Brazilian shelf based on grain size records. *The Holocene* 20, 863–875.
- Hammer, Ø., Harper, D., Ryan, P.D., 2001. PAST: paleontological statistics software package for education and data analysis. *Palaeontol. Electron.* 4.
- Hesp, P.A., Giannini, P.C.F., Martinho, C.T., Miot Da Silva, G., Asp Neto, N.E., 2009. The Holocene barrier system of the Santa Catarina coast, Southern Brazil. In: Dillenburg, S.R., Hesp, P.A. (Eds.), *Geology and Geomorphology of Holocene Coastal Barriers of Brazil*. Springer, Berlin – Heidelberg, pp. 93–134.
- Kanazawa, T., Sato, S., 2008. Environmental and physiological controls on shell microgrowth pattern of *Ruditapes philippinarum* (Bivalvia: Veneridae) from Japan. *J. Molluscan Stud.* 74, 89–95.
- Kjerfve, B., 1994. Coastal Lagoon Processes. Elsevier Oceanography Series/Elsevier Science.
- Ingram, B.L., Conrad, M.E., Ingle, J.C., 1996. Stable isotope and salinity systematics in estuarine waters and carbonates: San Francisco Bay. *Geochim. Cosmochim. Acta* 60 (3), 455–467.
- Lécuyer, C., Bodergat, A.-M., Martineau, F., Fourel, F., Gürbüz, K., Nazik, A., 2012. Water sources, mixing and evaporation in the Akyatan lagoon, Turkey. *Estuar. Coast. Shelf Sci.* 115, 200–209.
- Leonel, R.M.V., Magalhães, A.R.M., Lunetta, J.E., 1983. Sobrevivência de *Anomalocardia brasiliana* (Gmelin, 1791) (Mollusca: Bivalvia), em diferentes salinidades. *Boletim de Fisiologia Animal* 7, 63–72.
- Lima, T.A., Macario, K.D., Anjos, R.M., Gomes, P.R.S., Coimbra, M.M., Elmore, D., 2002. The antiquity of the prehistoric settlement of the central-south Brazilian coast. *Radiocarbon* 44 (3), 733–738.
- Lutz, R.A., Rhoads, D.C., 1977. Anaerobiosis and a theory of growth line formation. *Science* 198, 1222–1227.
- Luz, J.R., Boehs, G., 2011. Reproductive cycle of *Anomalocardia brasiliana* (Mollusca: Bivalvia: Veneridae) in the estuary of the Cachoeira River, Ilhéus, Bahia. *Braz. J. Biol.* 71, 679–686.
- Magrin, G., Gay García, G., Cruz Choque, D., Giménez, J.C., Moreno, A.R., Nagy, G.J., Nobre, C., Villamizar, A., 2007. Latin America. In: Parry, M.L., Canziani, O.F., Palutikof, J.P., van der Linden, P.J., Hanson, C.E. (Eds.), *Climate Change 2007: Impacts, Adaptation and Vulnerability. Contribution of working group II to the Fourth Assessment Report of the Intergovernmental Panel on Climate Change*. Cambridge University Press, Cambridge, UK, pp. 581–615.
- McConnaughey, T.A., Gillikin, D.P., 2008. Carbon isotopes in mollusk shell carbonates. *Geo-Mar. Lett.* 28, 287–299.
- Mannino, M.A., Thomas, K.D., Leng, M.J., Sloane, H.J., 2008. Shell growth and oxygen isotopes in the topshell *Osilinus turbinatus*: resolving past inshore sea surface temperatures. *Geo-Mar. Lett.* 28 (5/6), 309–325.
- Maoka, T., 2011. Carotenoids in marine animals. *Mar. Drugs* 9, 278–293.
- Meurer, A.Z., Netto, S.A., 2007. Seasonal dynamics of benthic communities in a shallow sublittoral site of Laguna Estuarine System (south, Brazil). *Braz. J. Aquat. Sci. Technol.* 11 (2), 53–62.
- Milano, S., Schöne, B.R., Witbaard, R., 2017. Changes of shell microstructural characteristics of *Cerastoderma edule* (Bivalvia) – a novel proxy for water temperature. *Palaeogeogr. Palaeoclimatol. Palaeoecol.* 465, 395–406.
- Miyaji, T., Tanabe, K., Schöne, B.R., 2007. Environmental controls on daily shell growth of *Phacosoma japonicum* (Bivalvia: Veneridae) from Japan. *Mar. Ecol. Prog. Ser.* 336, 141–150.
- Mohan, J.A., Walther, B.D., 2014. Spatiotemporal variation of trace elements and stable isotopes in subtropical estuaries: II. Regional, local, and seasonal salinity-element relationships. *Estuar. Coasts* 38, 769–781.
- Monti, D., Frenkiel, L., Moueza, M., 1991. Demography and growth of *Anomalocardia brasiliana* (Gmelin) (Bivalvia: Veneridae) in a mangrove in Guadalupe (French West Indies). *J. Molluscan Stud.* 57, 249–257.
- Mook, W.G., Tan, F.C., 1991. Stable carbon isotopes in rivers and estuaries. In: Degens, E.T., Kempe, S., Richey, J.E. (Eds.), *Biogeochemistry of Major World Rivers*. Scope, pp. 245–264.
- Norkko, A., Thrush, S.F., Hewitt, J.E., Cummings, V.J., Norkko, J., Ellis, J.L., Funnell, G.A., Schultz, D., MacDonald, I., 2002. Smothering of estuarine sandflats by terrigenous clay: the role of wind-wave disturbance and bioturbation in site-dependent macrofaunal recovery. *Mar. Ecol. Prog. Ser.* 234, 23–42.
- O'Leary, M.H., 1988. Carbon isotopes in photosynthesis: fractionation techniques may reveal new aspects of carbon dynamics in plants. *Bioscience* 38, 328–336.
- Orselli, J., 1986. *Climatologia*. Gaplan – SC. Atlas de Santa Catarina. Aerofoto Cruzeiro, Rio de Janeiro, pp. 38–39.
- Osório, F.H.T., Silva, L.F.O., Piancini, L.D.S., Azevedo, A.C.B., Liebel, S., Yamamoto, F.Y., Philippi, V.P., Oliveira, M.L.S., Ortolani-Machado, C.F., Filipak Neto, F., Cestari, M.M., da Silva de Assis, H.C., de Oliveira Ribeiro, C.A., 2014. Water quality assessment of the Tubarão River through chemical analysis and biomarkers in the neotropical fish *Geophagus brasiliensis*. *Environ. Sci. Pollut. Res. Int.* 21, 9145–9160.
- Prendergast, A.L., Azzopardi, M., O'Connell, T.C., Hunt, C., Barker, G., Stevens, R.E., 2013. Oxygen isotopes from *Phorcus (Osilinus) turbinatus* shells as a proxy for sea surface temperature in the central Mediterranean: a case study from Malta. *Chem. Geol.* 345, 77–86.
- Peel, M.C., Finlayson, B.L., McMahon, T.A., 2007. Updated world map of the Köppen-Geiger climate classification. *Hydrol. Earth Syst. Sci.* 11, 1633–1644.
- Peterson, C.H., 1985. Patterns of lagoonal bivalve mortality after heavy sedimentation and their paleoecological significance. *Paleobiology* 11, 139–159.
- Poulain, C., Lorrain, A., Mas, R., Gillikin, D.P., Dehairs, F., Robert, R., Paulet, Y.-M., 2010. Experimental shift of diet and DIC stable carbon isotopes: influence on shell $\delta^{13}\text{C}$ values in the Manila clam *Ruditapes philippinarum*. *Chem. Geol.* 272, 75–82.
- Raia, A., Cavalcanti, I.F.A., 2008. The life cycle of the South American monsoon system. *J. Clim.* 21, 6227–6246.
- Rios, E.C., 1994. *Seashells of Brazil*. 492. Editora da Fundação Universidade do Rio Grande, Rio Grande.
- Rodrigues, A.M.L., Borges-Azevedo, C.M., Costa, R.S., Henry-Silva, G.G., 2013. Population structure of the bivalve *Anomalocardia brasiliana* (Gmelin, 1791) in the semi-arid estuarine region of northeastern Brazil. *Braz. J. Biol.* 73, 819–833.
- Schaeffer-Novelli, Y., Cintrón-Molero, G., Adaipe, R.R., de Camargo, T.M., 1990. Variability of mangrove ecosystems along the Brazilian coast. *Estuaries* 13, 204–218.
- Scheel-Ybert, R., 2001. Man and vegetation in southeastern Brazil during the Late Holocene. *J. Archaeol. Sci.* 28, 471–480.
- Schöne, B.R., 2003. A 'clam-ring' master-chronology 30 constructed from a short-lived bivalve 31 mollusk from the northern gulf of 32 California, USA. *The Holocene* 13 (1), 39–49.
- Schöne, B.R., 2013. *Arctica islandica* (Bivalvia): a unique paleoenvironmental archive of the northern North Atlantic Ocean. *Glob. Planet. Change* 111, 199–225.
- Schöne, B.R., Dunca, E., Fiebig, J., Pfeiffer, M., 2005. Mutvei's solution: an ideal agent for resolving microgrowth structures of biogenic carbonates. *Palaeogeogr. Palaeoclimatol. Palaeoecol.* 228, 149–166.
- Schöne, B.R., 2008. The curse of physiology—challenges and opportunities in the interpretation of geochemical data from mollusk shells. *Geo-Mar. Lett.* 28, 269–285.
- Schöne, B.R., Surge, D.M., 2012. Bivalve Sclerochronology and Geochemistry. In: Seldon, P., Hardesty, J. (Eds.), *Part N, Bivalvia, Revised, Volume 1. Treatise Online, Chapter: 14*. Publisher: Paleontological Institute 46. Paleontological Institute, pp. 1–24.

- Schöne, B.R., Gillikin, D.P., 2013. Unravelling environmental histories from skeletal diaries – advances in sclerochronology. *Palaeogeogr. Palaeoclimatol. Palaeoecol.* 373, 1–5.
- Silva-Cavalcanti, J., Costa, M., 2011. Fisheries of *Anomalocardia brasiliana* in tropical estuaries. *Panam. J. Aquat. Sci.* 6, 86–99.
- Soares, M.L.G., Estrada, G.C.D., Fernandez, V., Tognella, M.M.P., 2012. Southern limit of the Western South Atlantic mangroves: assessment of the potential effects of global warming from a biogeographical perspective. *Estuar. Coast. Shelf Sci.* 101, 44–53.
- Sonnerup, R.E., Quay, P.D., McNichol, A.P., Bullister, J.L., Westby, T.A., Anderson, H.L., 1999. Reconstructing the oceanic ^{13}C Suess effect. *Glob. Biogeochem. Cycles* 13, 857–872.
- Stenseth, N.C., Mysterud, A., Ottersen, G., Hurrell, J.W., Chan, K.-S., Lima, M., 2002. Ecological effects of climate fluctuations. *Science* 297, 1292–1296.
- Surge, D.M., Lohmann, K.C., Goodfriend, G.A., 2003. Reconstructing estuarine conditions: oyster shells as recorders of environmental change, Southwest Florida. *Estuar. Coast. Shelf Sci.* 57, 737–756.
- Taylor, J.D., Kennedy, W.J., Hall, A., 1973. The shell structure and mineralogy of the Bivalvia. II Lucinacea-Clavagellacea, conclusions. *Bulletin of the British Museum (natural history). Zoology* 22, 255–294.
- Tognella, M.M.P., Soares, M.L.G., Cuevas, E., Medina, E., 2016. Heterogeneity of elemental composition and natural abundance of stable isotopes of C and N in soils and leaves of mangroves at their southernmost West Atlantic range. *Braz. J. Biol.* <http://dx.doi.org/10.1590/1519-6984.05915>.
- Torrence, C., Compo, G.P., 1998. A practical guide to wavelet analysis. *Bull. Am. Meteorol. Soc.* 79, 61–78.
- Urmos, J., Sharma, S.K., Mackenzie, F.T., 1991. Characterization of some biogenic carbonates with Raman spectroscopy. *Am. Mineral.* 76, 641–646.
- Vera, C.S., Vigliarolo, P.K., Berbery, E.H., 2002. Cold season synoptic-scale waves over subtropical South America. *Mon. Weather Rev.* 130, 684–699.
- Villagran, X.S., Klokler, D., Peixoto, S., DeBlasis, P.A.D., Giannini, P.C.F., 2011. Building coastal landscapes: zooarchaeology and geoarchaeology of Brazilian shell mounds. *J. Isl. Coast. Archaeol.* 6, 211–234.
- Villagran, X., 2014. A redefinition of waste: deconstructing shell and fish mound formation among coastal groups of southern Brazil. *J. Anthropol. Archaeol.* 36, 211–227.
- Wanamaker Jr., A.D., Kreutz, K.J., Schöne, B.R., Maasch, K.A., Pershing, A.J., Borns, H.W., Introne, D.S., Feindel, S., 2008. A late Holocene paleo-productivity record in the western gulf of Maine, USA, inferred from growth histories of the long-lived ocean quahog (*Arctica islandica*). *Int. J. Earth Sci.* 98, 19–29.
- Withnall, R., Chowdhry, B.Z., Silver, J., Edwards, H.G.M., de Oliveira, L.F.C., 2003. Raman spectra of carotenoids in natural products. *Spectrochim. Acta A Mol. Biomol. Spectrosc.* 59, 2207–2212.
- Yan, L., Schöne, B.R., Arkhipkin, A., 2012. *Eurhomalea exalbida* (Bivalvia): a reliable recorder of climate in southern South America? *Palaeogeogr. Palaeoclimatol. Palaeoecol.* 350–352, 91–100.